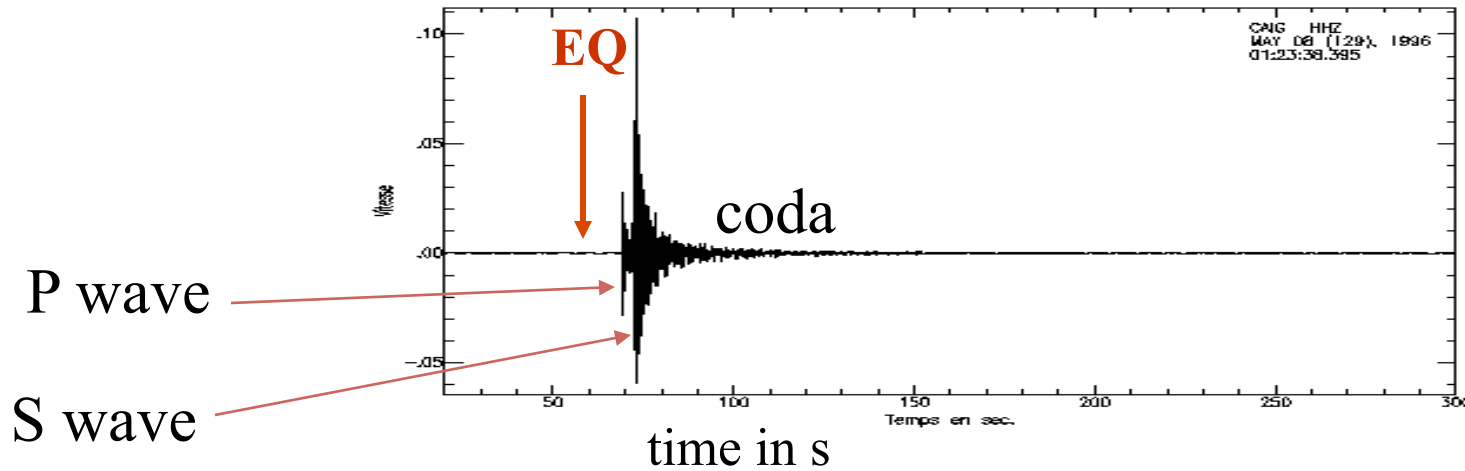


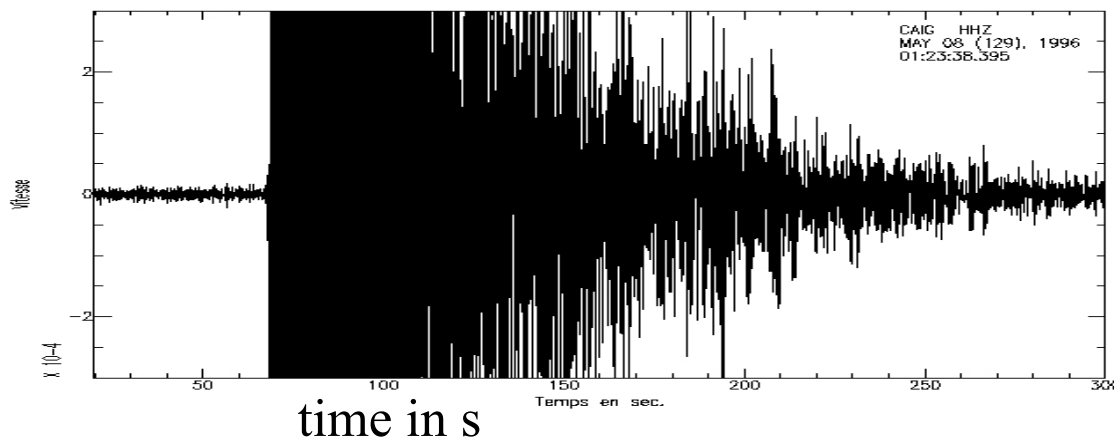
1. Seismograms: ballistic waves, coda, ambient noise.
2. Green function and correlations
3. Imaging: surface waves and body waves. Applications.
4. Monitoring: sensitivity of direct and scattered waves. Applications.

Analysis of continuous records

Example of a record of a local earthquake in the band .5-20Hz



scale x 1000:

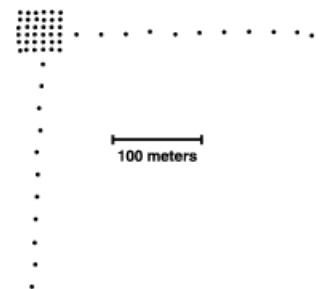
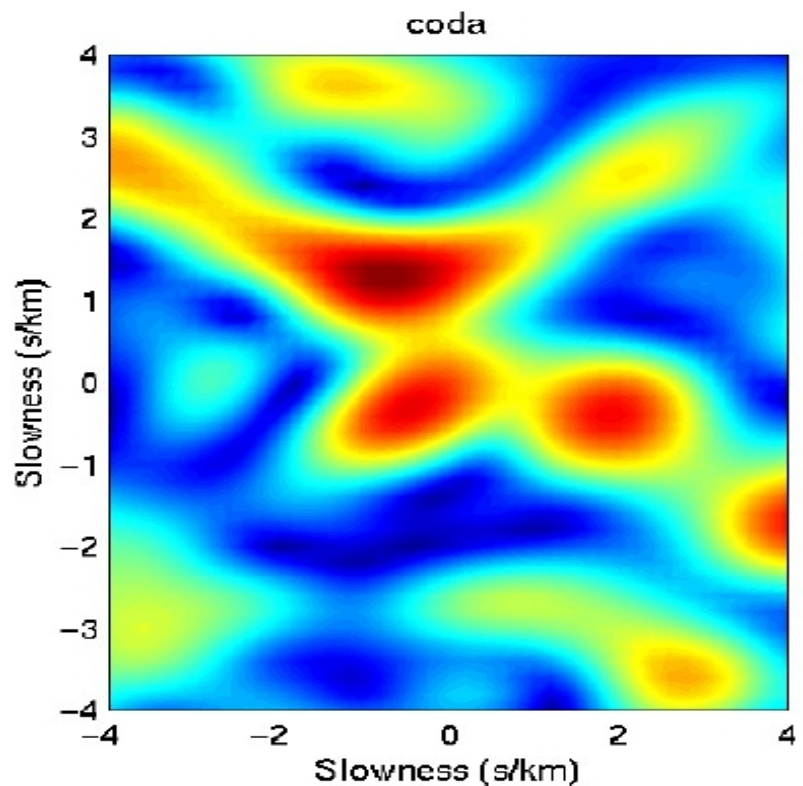
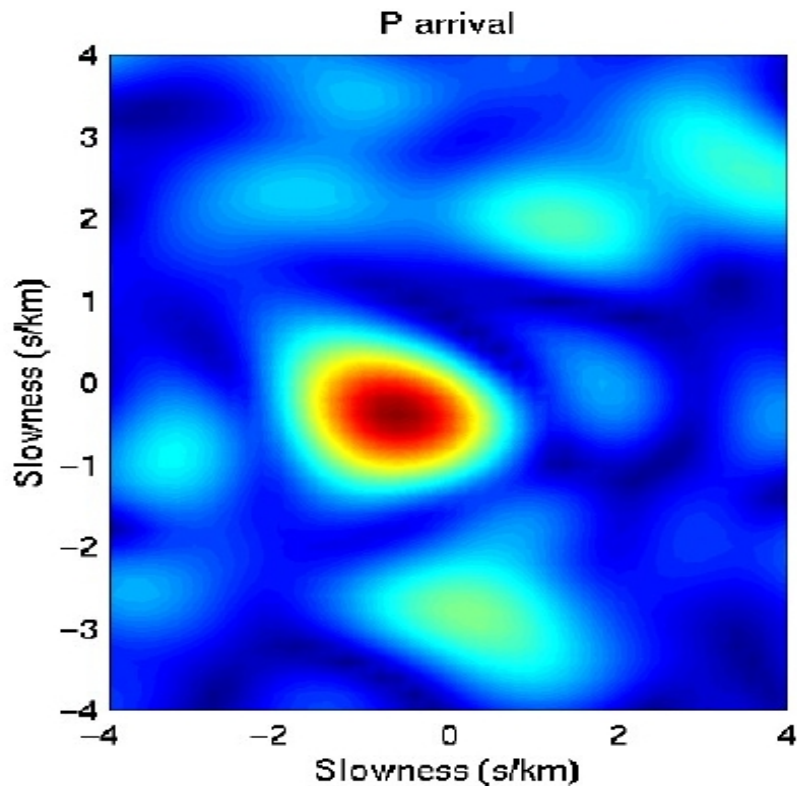


Coda: tail, end of a piece of music....

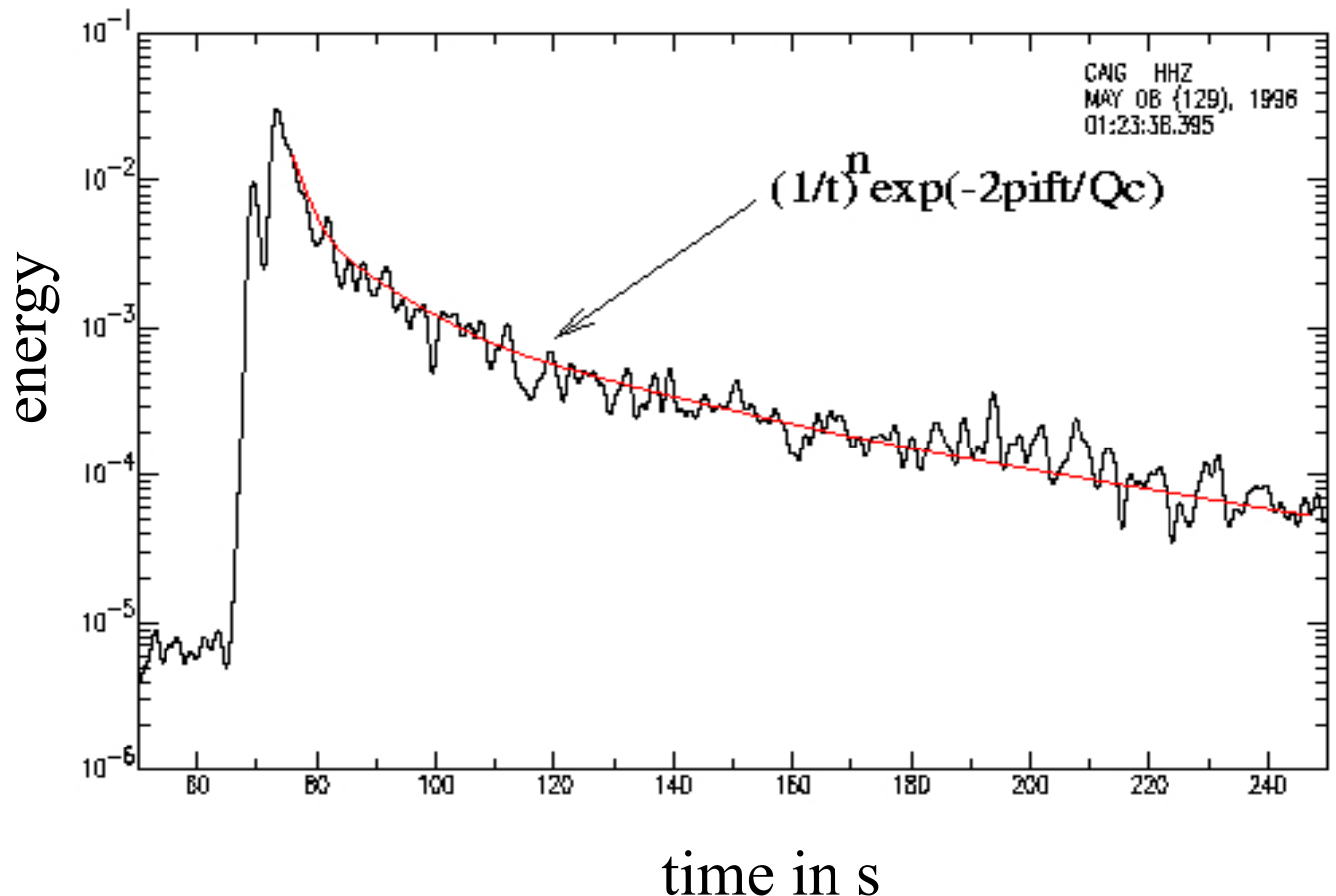
Frequency-wavenumber analysis

(Pinon Flat Seismometer Array)

$$u(x,y) \rightarrow u(k_x, k_y)$$

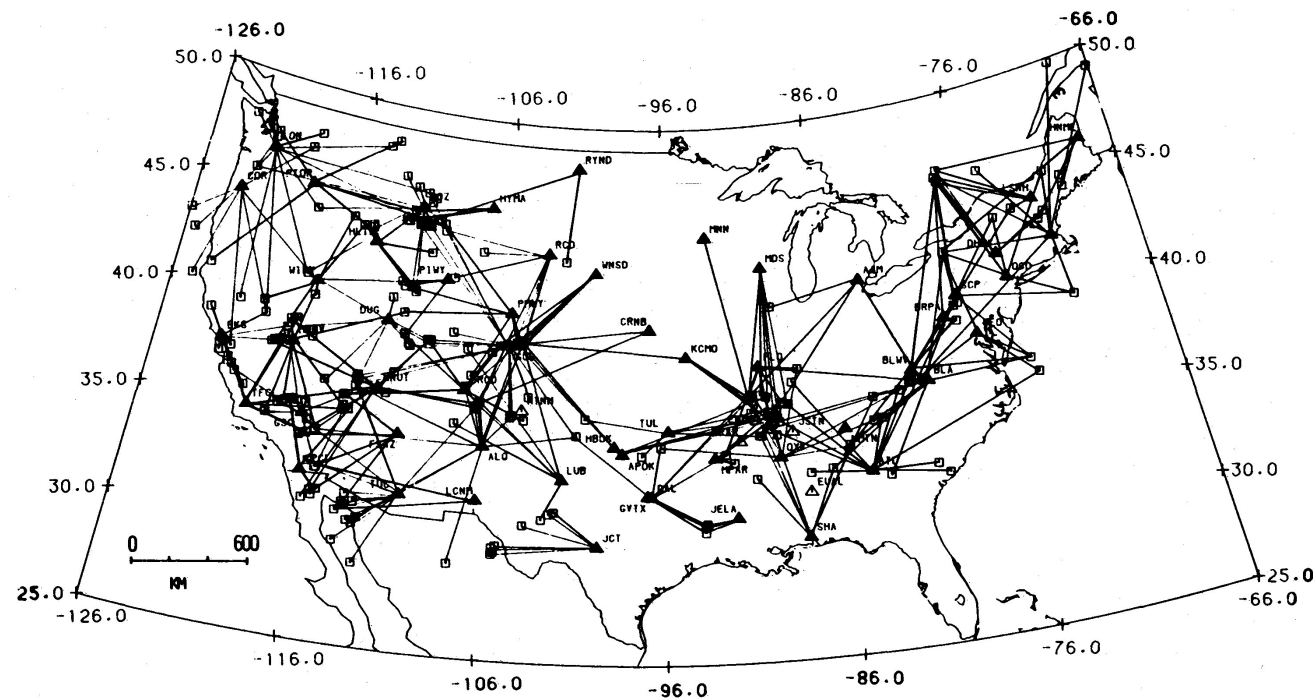


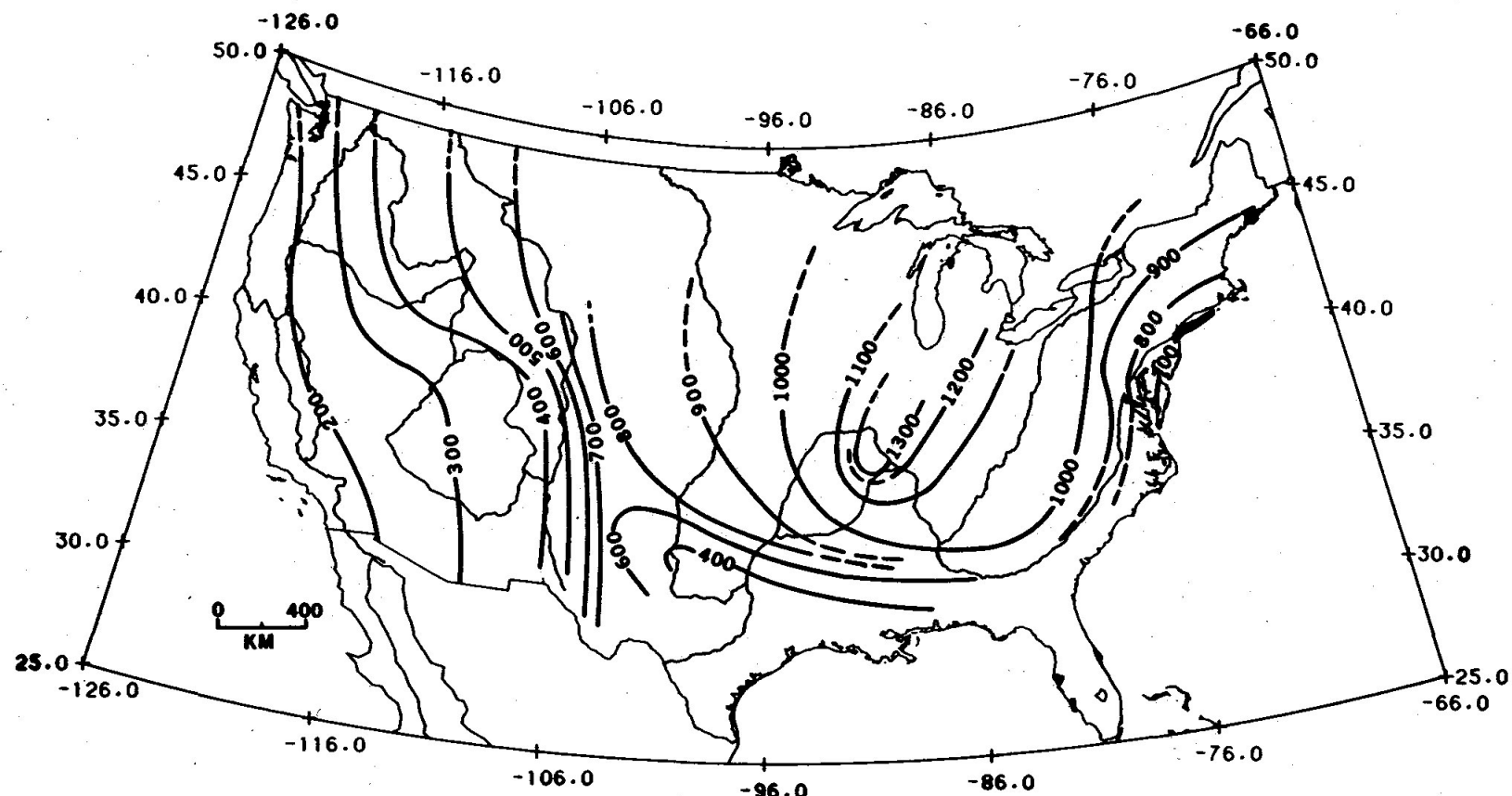
Energy decay in the coda (Aki and Chouet, 1975)



The decay is constant in a region, independently of source and receiver: Q_{coda}

Coda Q in US (Singh and Herrmann, 1983)





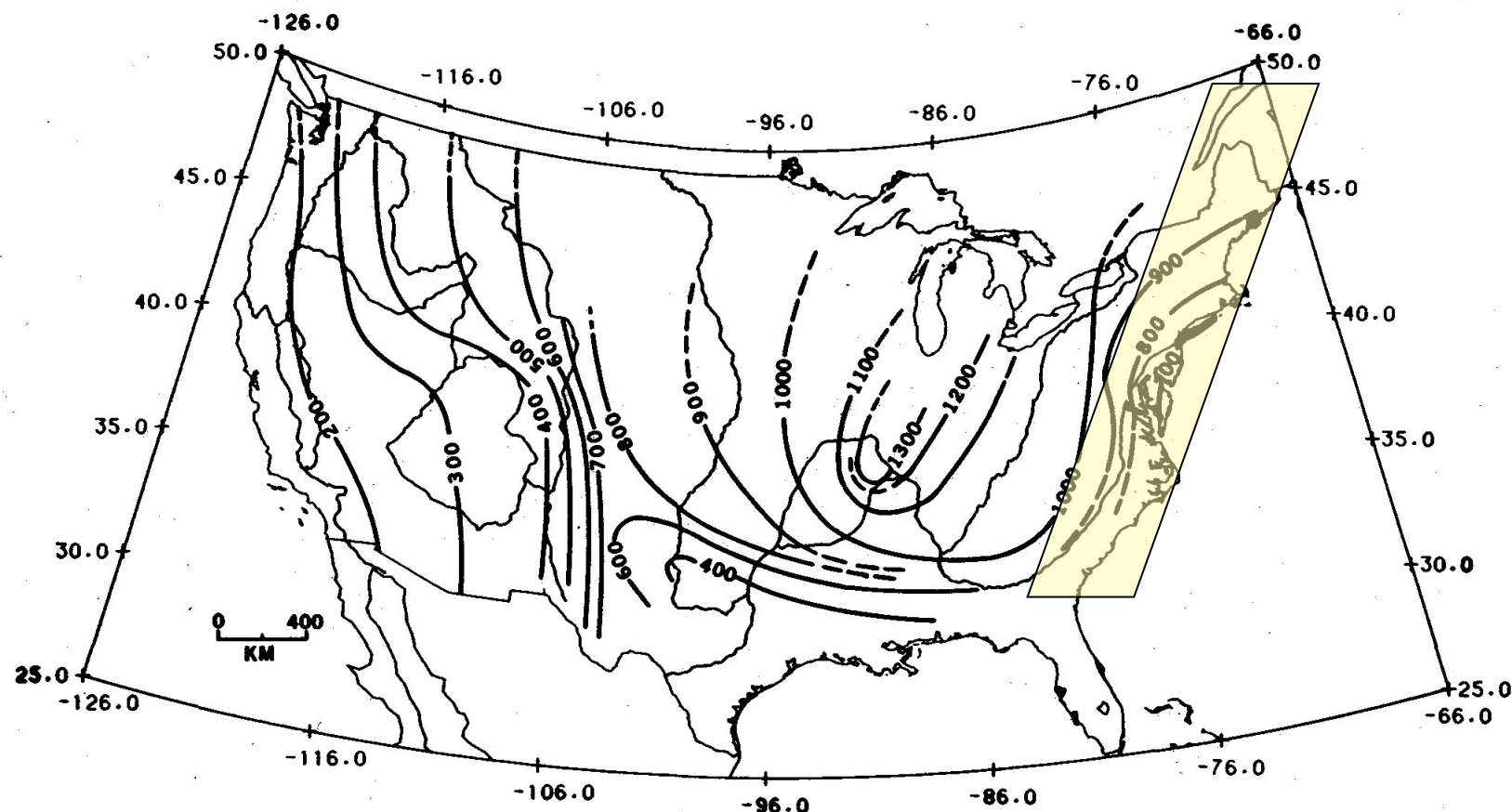


Fig. 15. Contour map of coda Q_0 for the entire continental United States.

Appalachian (Hercynian) belt : $Q_c \sim 600$

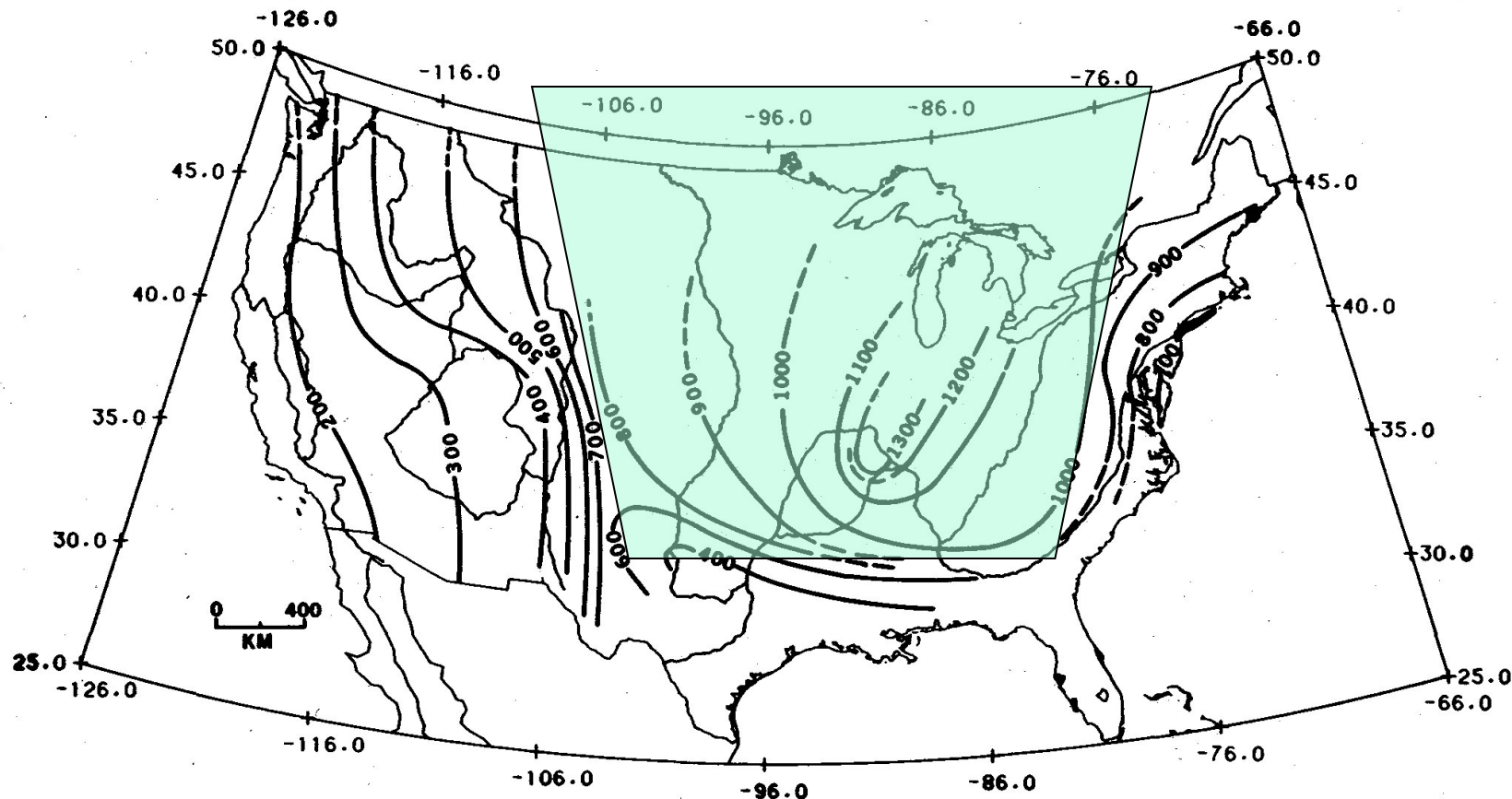


Fig. 15. Contour map of coda Q_0 for the entire continental United States.

Central shield : $Q_c \sim 1000$

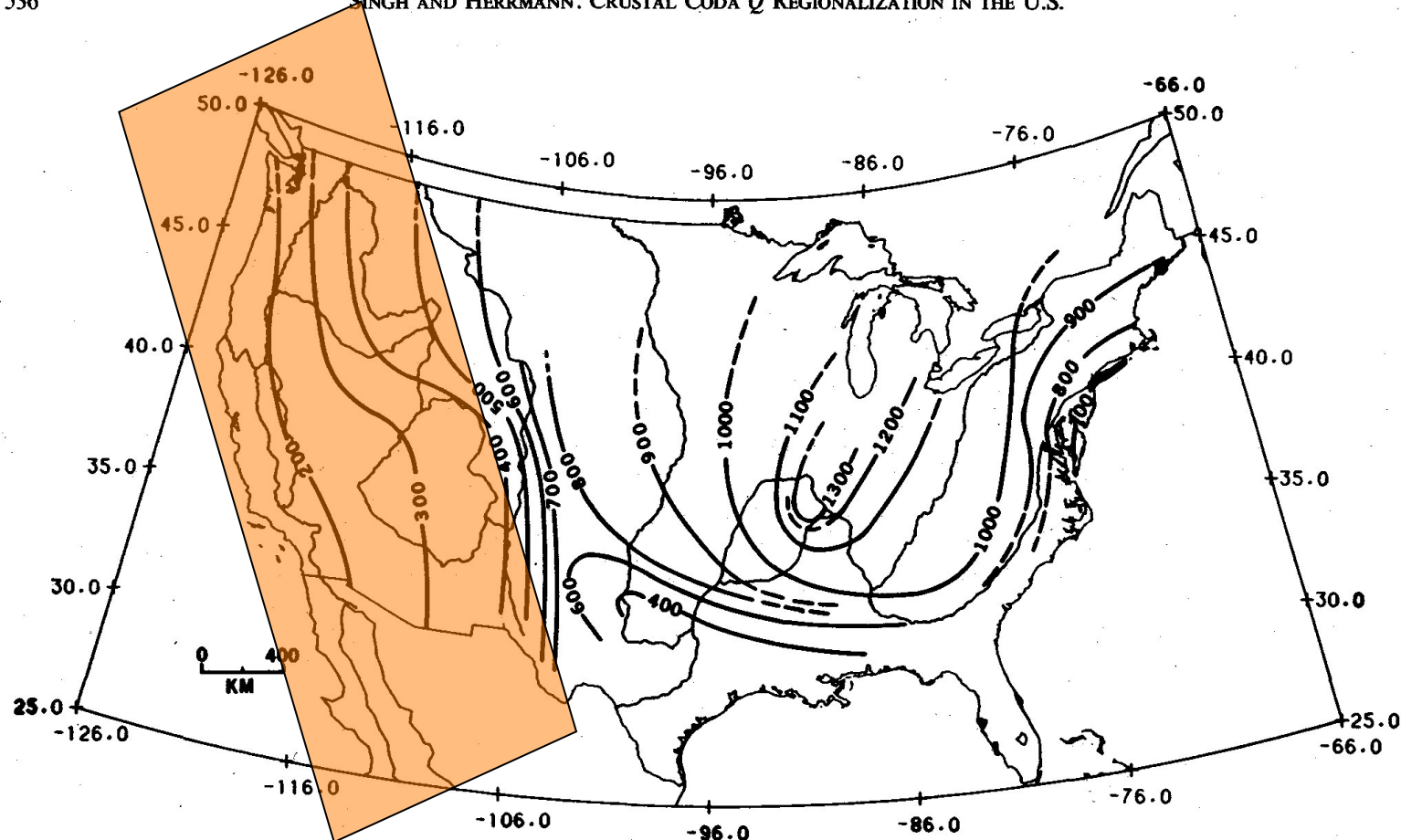
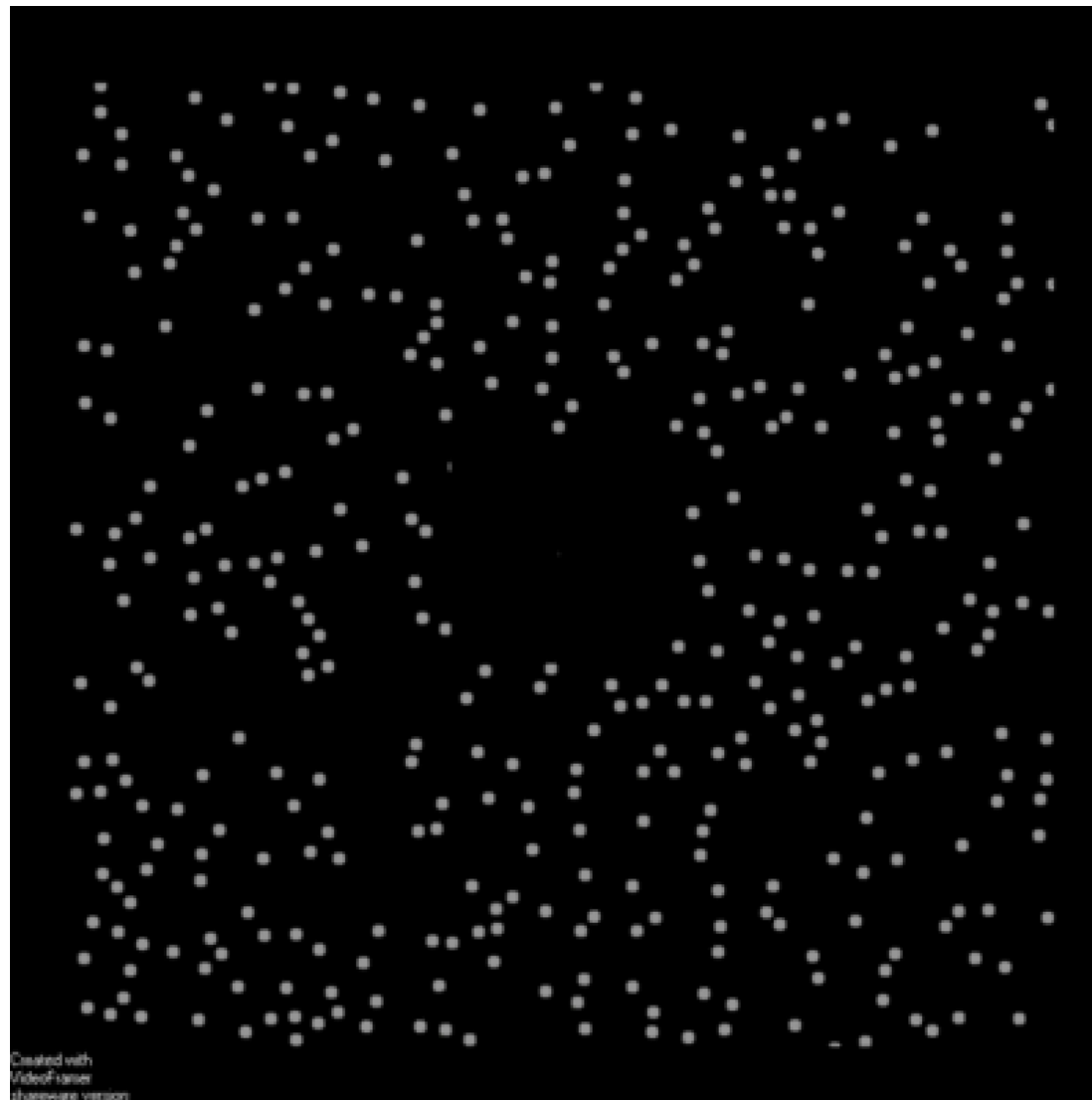


Fig. 15. Contour map of coda Q_0 for the entire continental United States.

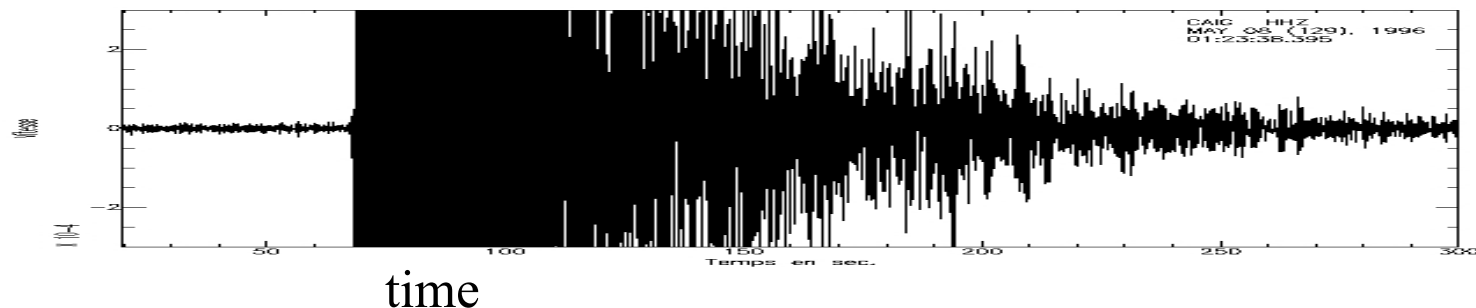
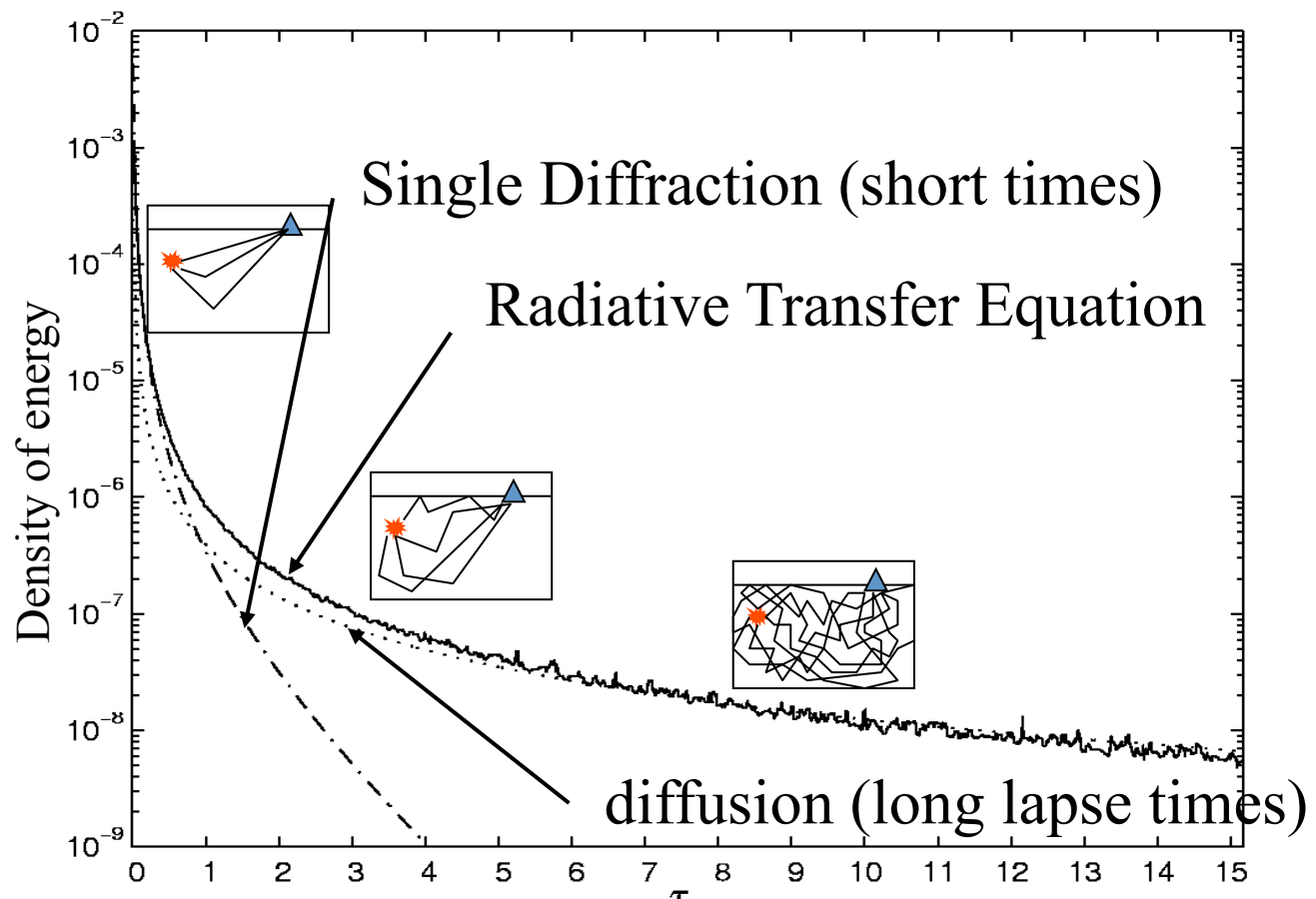
Tectonically active western US: $Q_c=100-300$

Transient signals in a complex medium.....



Created with
VideoFramer
shareware version

Propagation regimes and description of energy



The Diffusion Approximation

General Idea:

- Each scattering distributes energy over all space directions
- After several scatterings the intensity becomes almost isotropic

$$I(t, \vec{r}, \vec{\Omega}) = \text{Angularly Averaged Intensity} + \\ \text{constant} \times \vec{J}(t, \vec{r}) \cdot \vec{\Omega}$$

The current density $\vec{J}(\vec{r}, t)$, points in the direction of maximum energy flow.
Integrating the RT Eq over all space directions leads to:

$$\partial_t \rho(t, \vec{r}) - D \nabla^2 \rho(t, \vec{r}) = \delta(t, \vec{r})$$

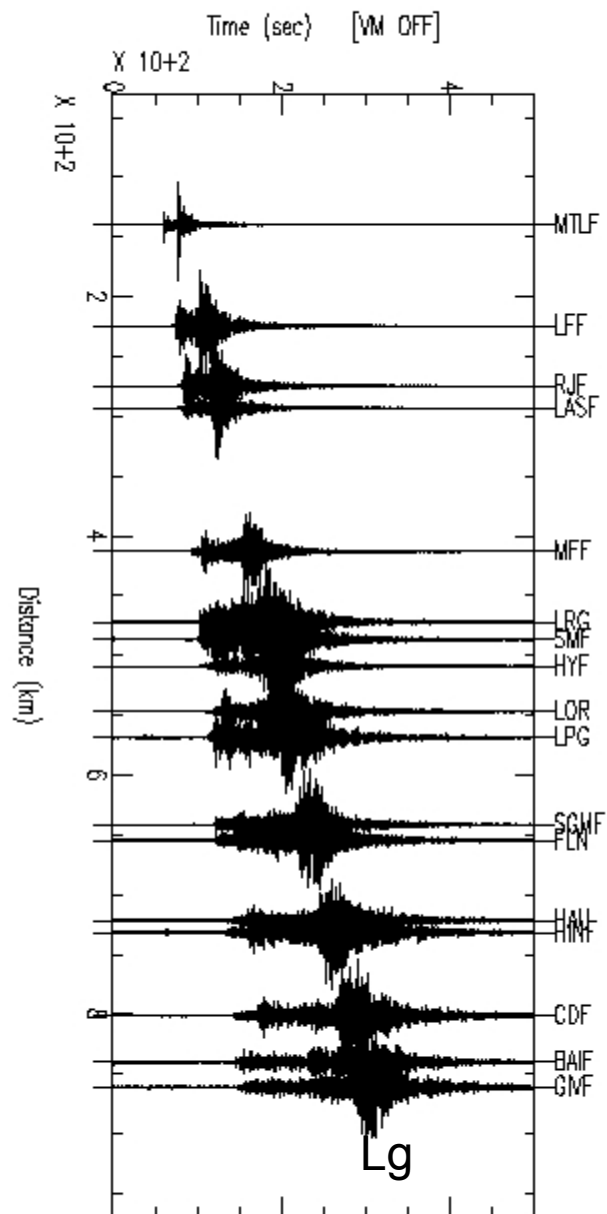
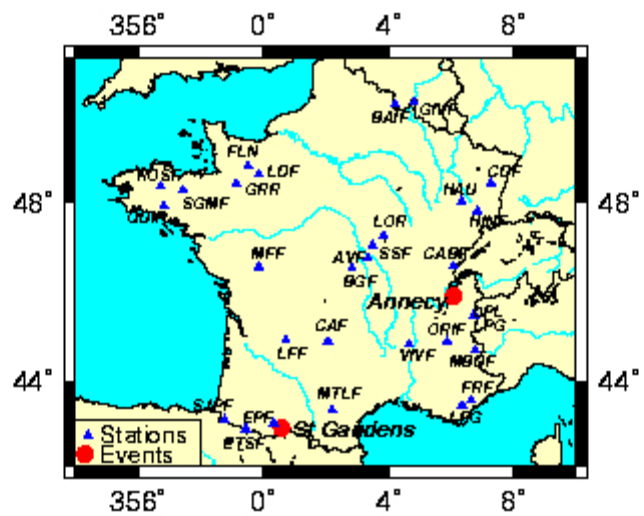
where ρ is the local energy density.

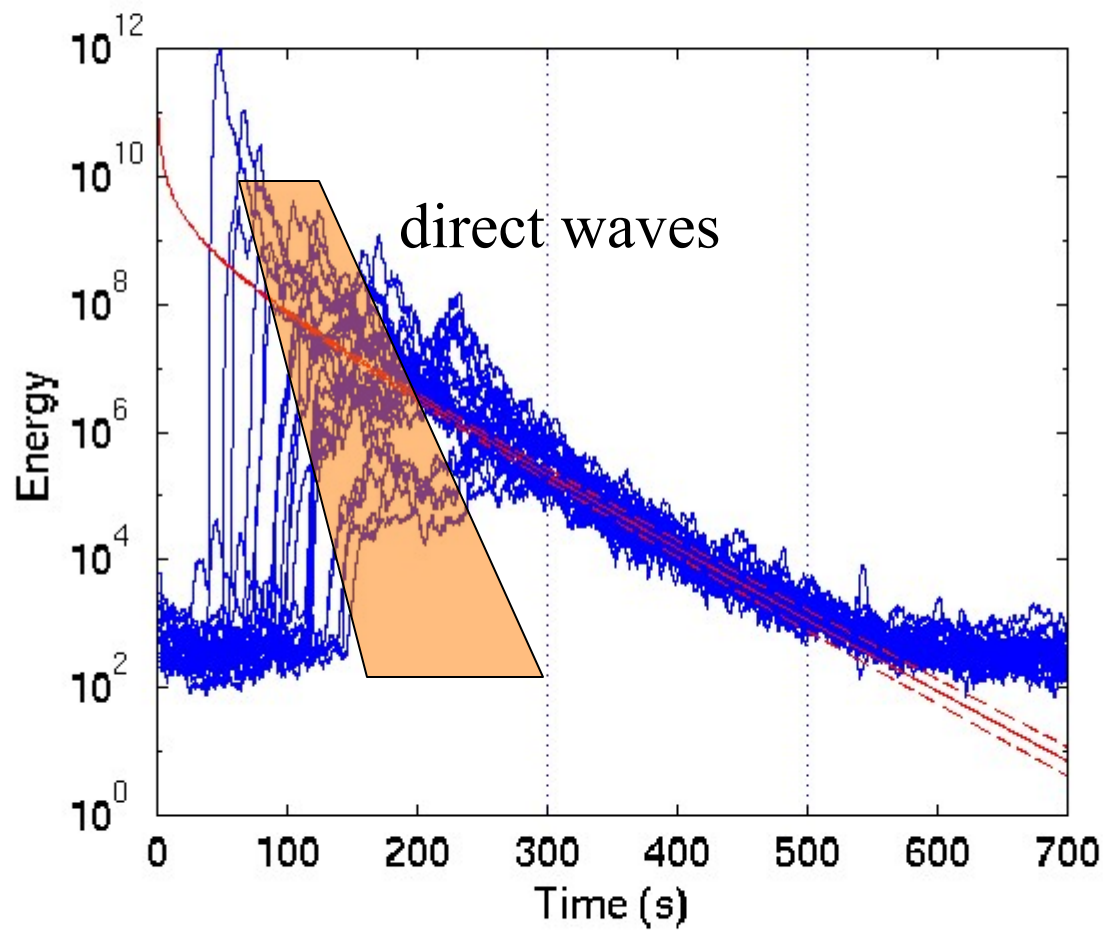
$$\rho(\vec{r}, \vec{r}', t) = \frac{1}{(4\pi Dt)^{d/2}} e^{-|\vec{r}-\vec{r}'|^2/4Dt}$$

$$\rho(t, \vec{r}) \sim \frac{1}{(Dt)^{3/2}} \text{ for large } t.$$

$D = vl/3$ is the diffusion constant of the waves.

Regional seismograms





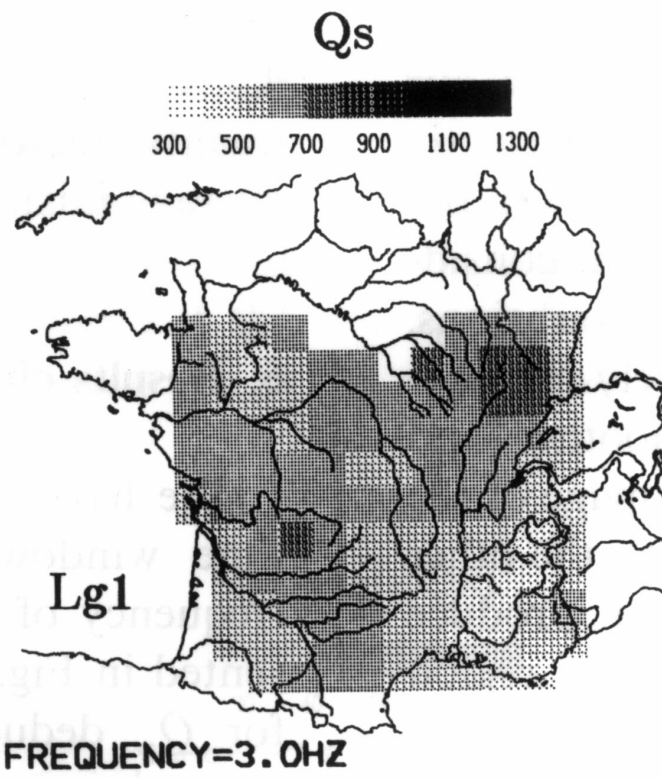
Rapid decay with distance

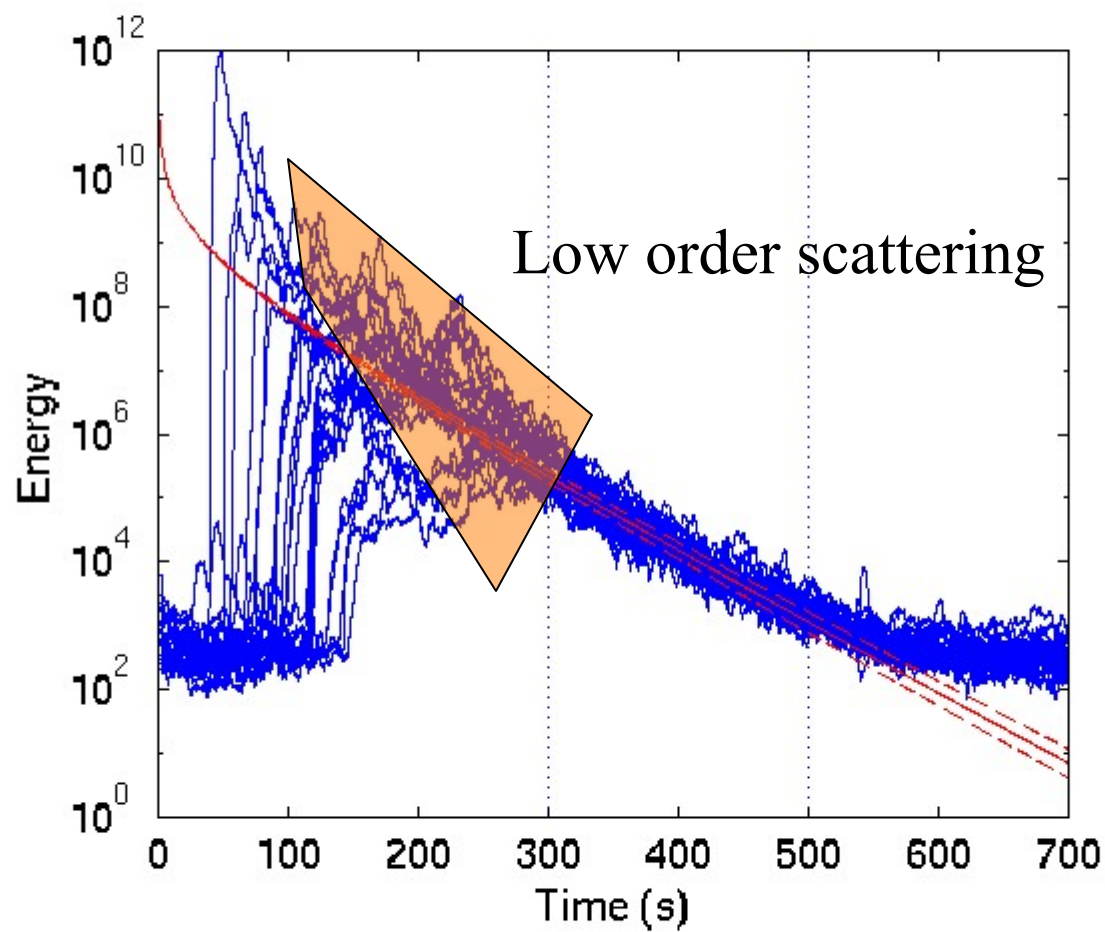


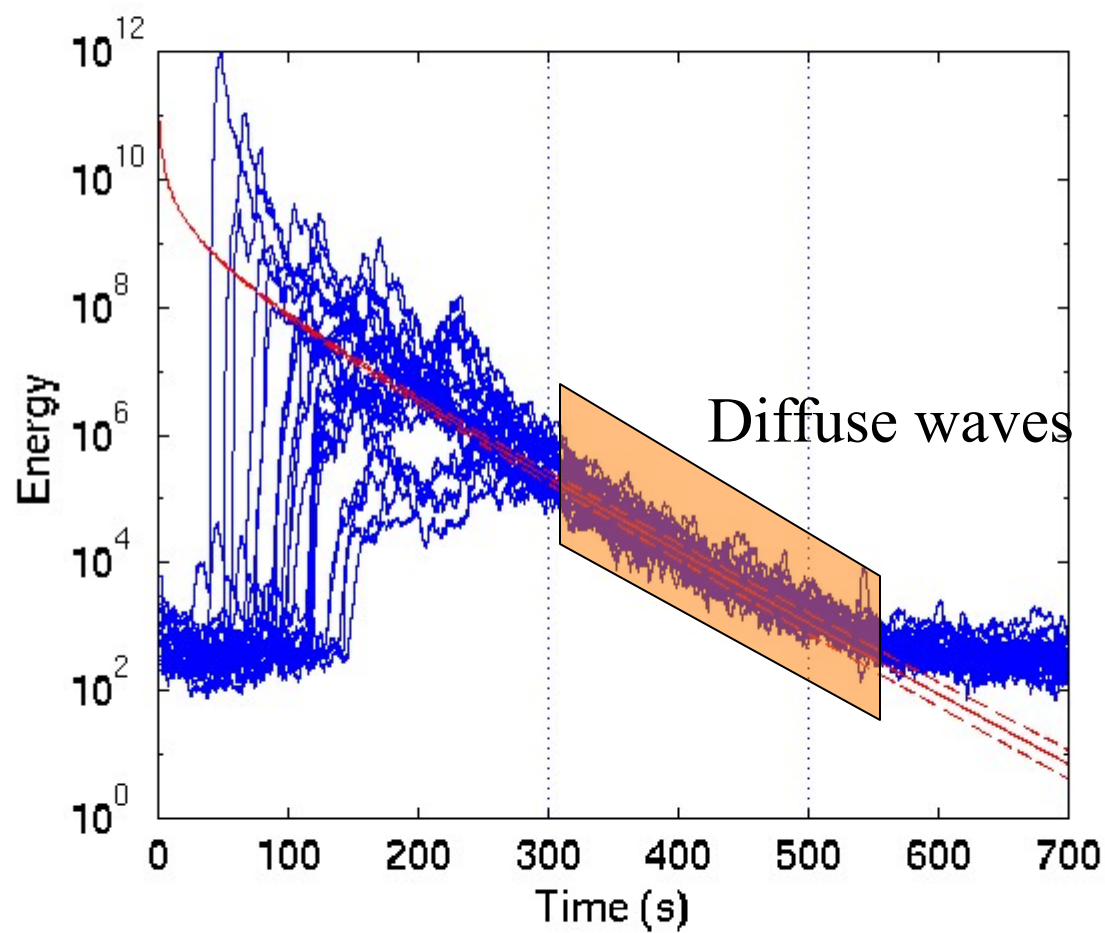
Observations:

$$l_{\text{total}} \text{ (km)} = 160 / f^{1/2} \text{ for S waves}$$

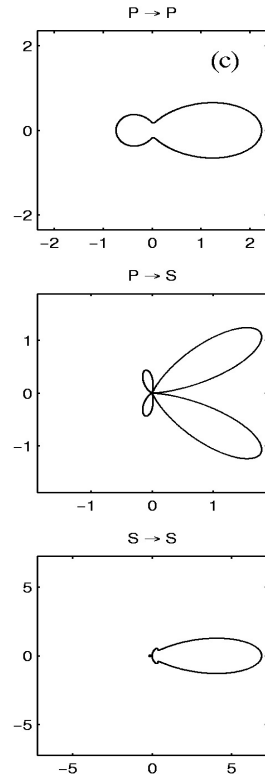
$$1/l_{\text{total}} = 1/l_S + 1/l_A$$



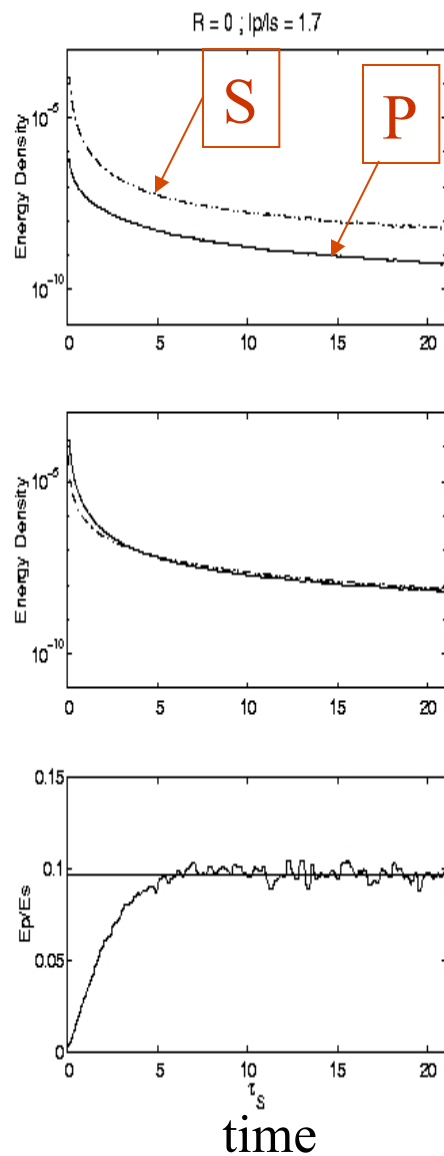




Cross sections

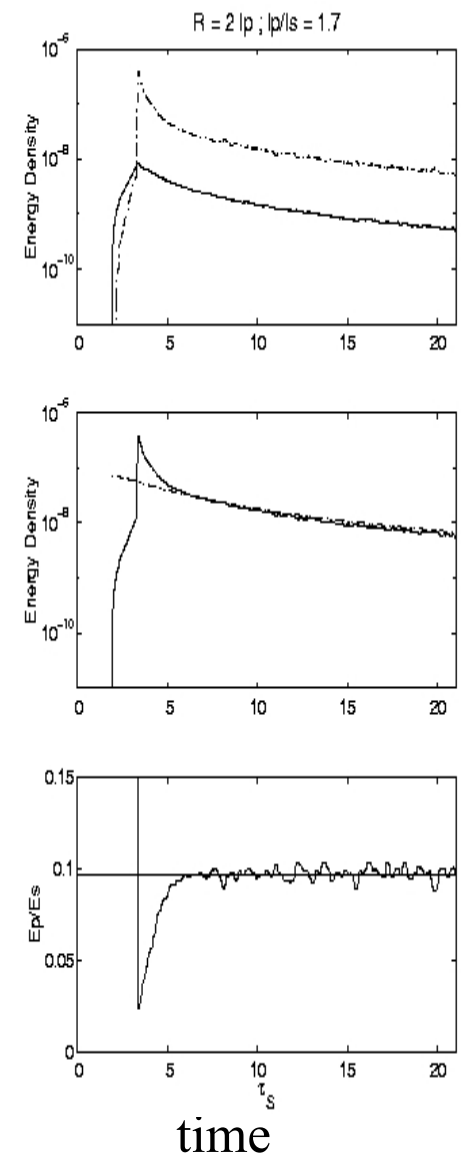


$ka=1.6$



total energy
vs
diffusion app.

Energy ratio

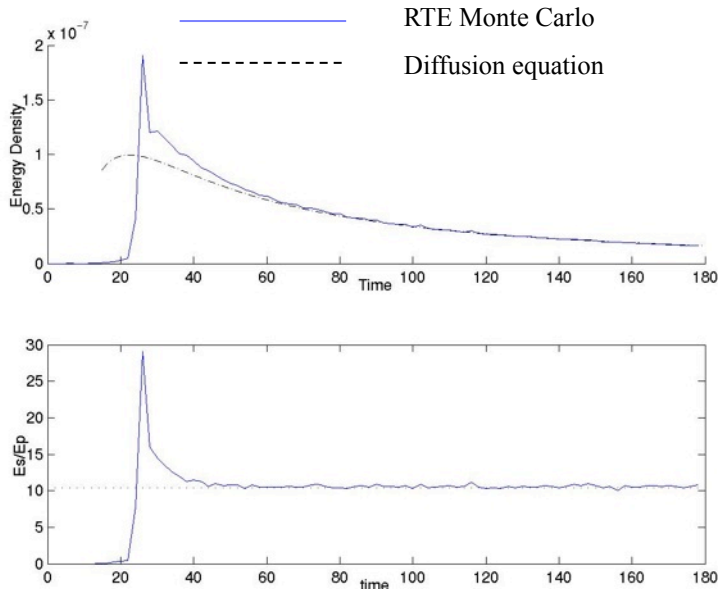


Searching for a marker of the regime of scattering...

Equipartition principle for a completely randomized (diffuse) wave-field: in average, all the modes of propagation are excited to equal energy.

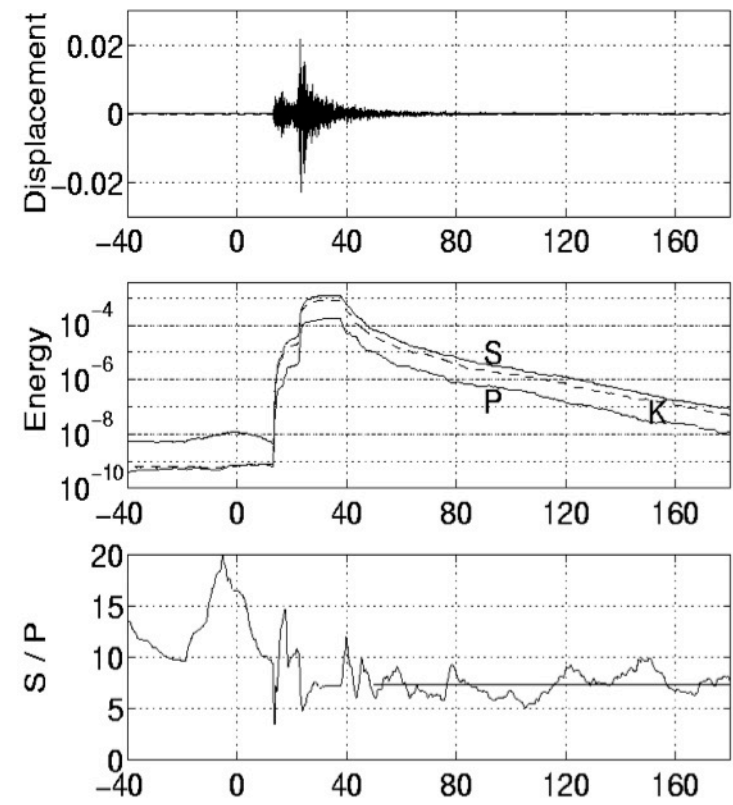
Implication for elastic waves (Weaver, 1982, Ryzhik et al., 1996): P to S energy ratio stabilizes at a value independant of the details of scattering!

Numerical simulation



Observations

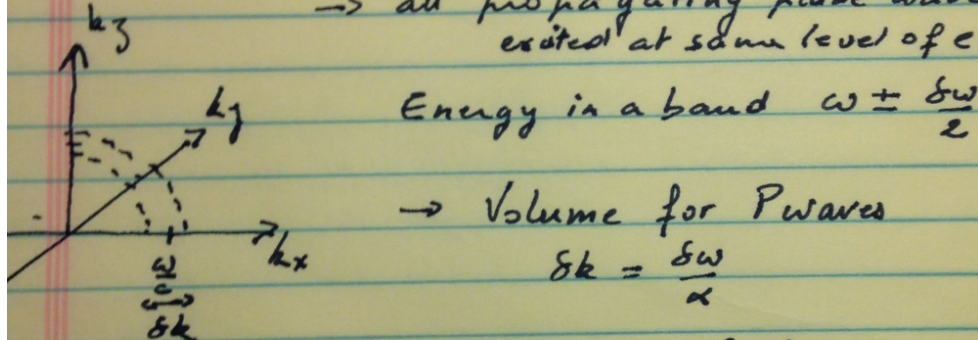
Event 11



Partition of energy (Full elastic space)

Multiphase scattering, large t
 → "equipartition"
 [reference medium + disorder]

Phase space of the full space elastic problem
 → all propagating plane waves
 excited at same level of energy



→ Volume for P-waves

$$\delta k = \frac{\delta\omega}{\alpha}$$

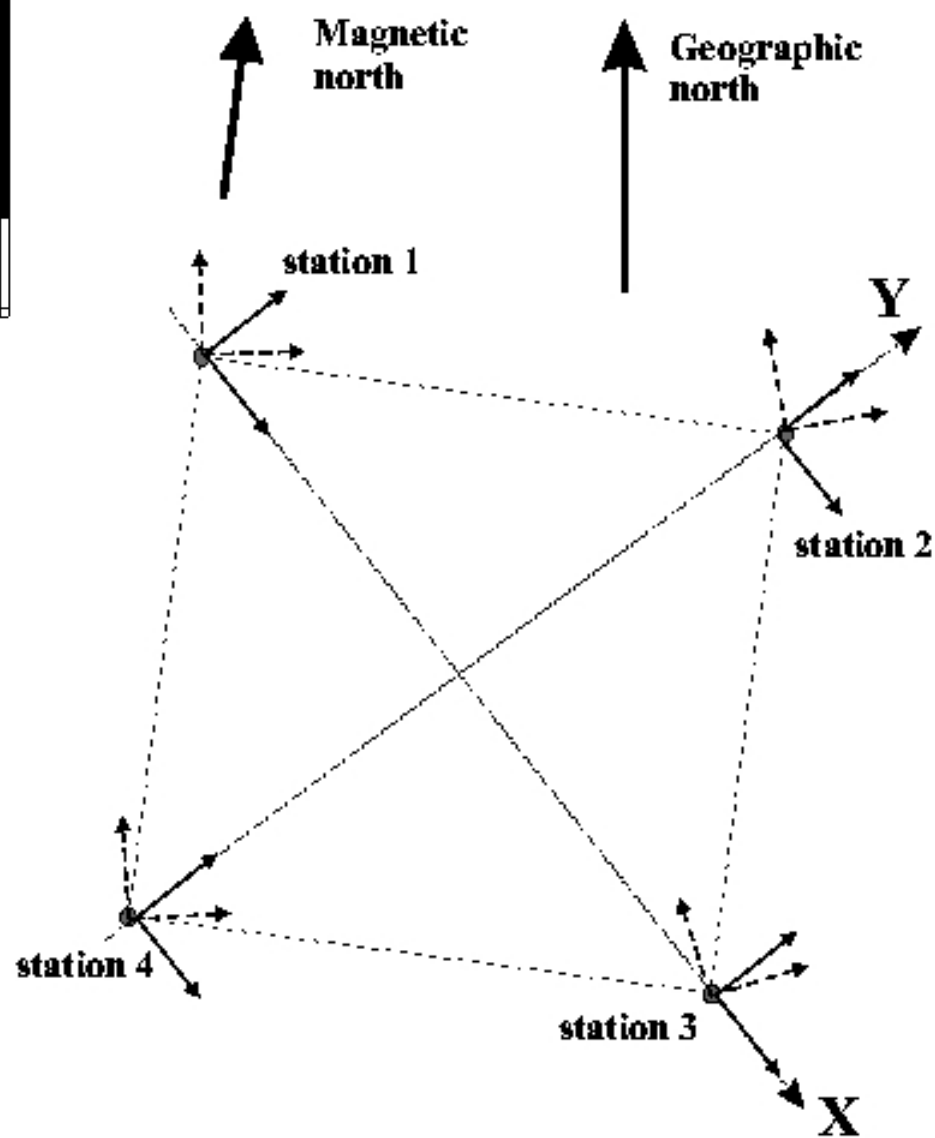
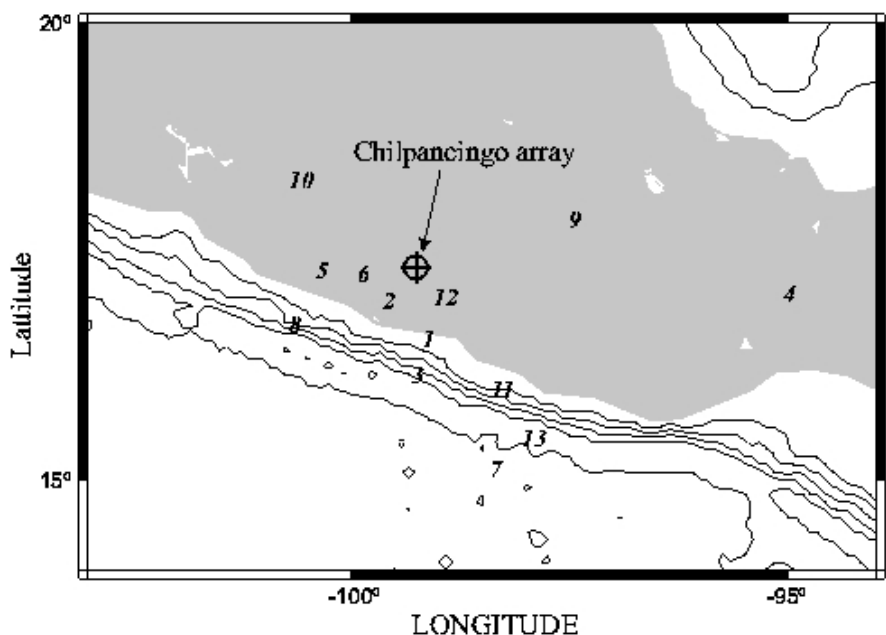
$$V_p = 4\pi \left(\frac{\omega}{\alpha}\right)^2 \frac{\delta\omega}{\alpha} = 4\pi \delta\omega \omega \frac{1}{\alpha^3}$$

Volume for each S polarisation: $V_{SH/SV} = 4\pi \delta\omega \omega \frac{1}{\beta^3}$

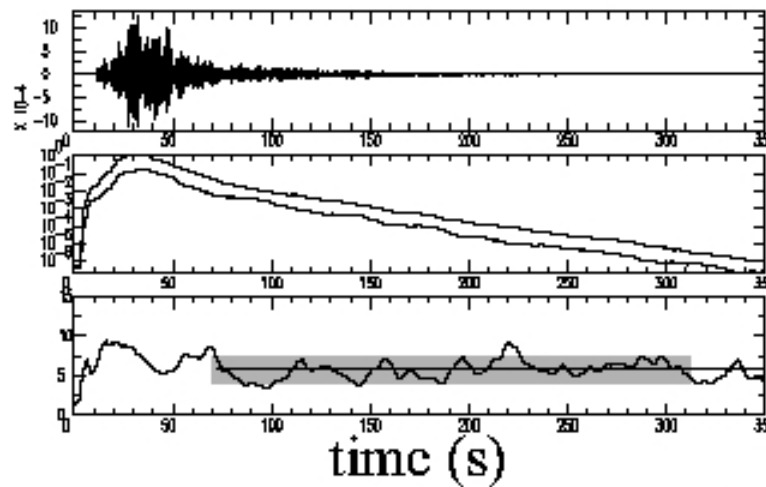
$$\Rightarrow V_S = 2 \times 4\pi \delta\omega \omega \frac{1}{\beta^3}$$

$$\text{Equal excitation} \Rightarrow \frac{E_S}{E_p} = \frac{V_S}{V_p} = 2 \frac{\alpha^3}{\beta^3}$$

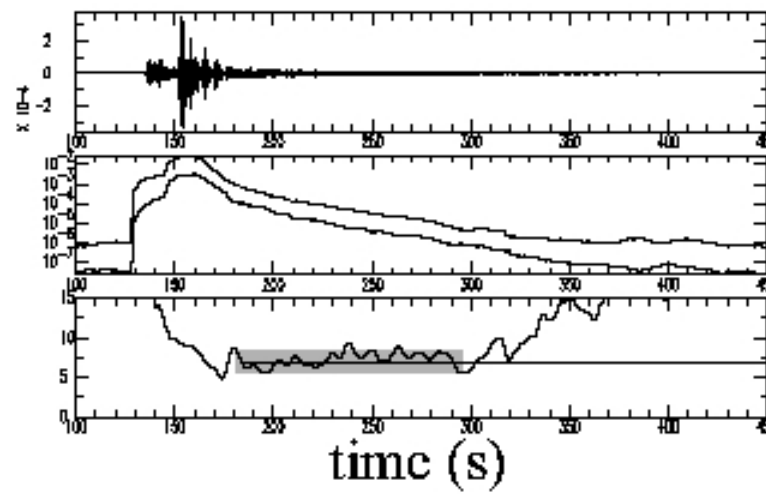
[Note $\alpha = \beta \Rightarrow \frac{E_S}{E_p} \approx 10.4 \Rightarrow$ see numerical simulation]

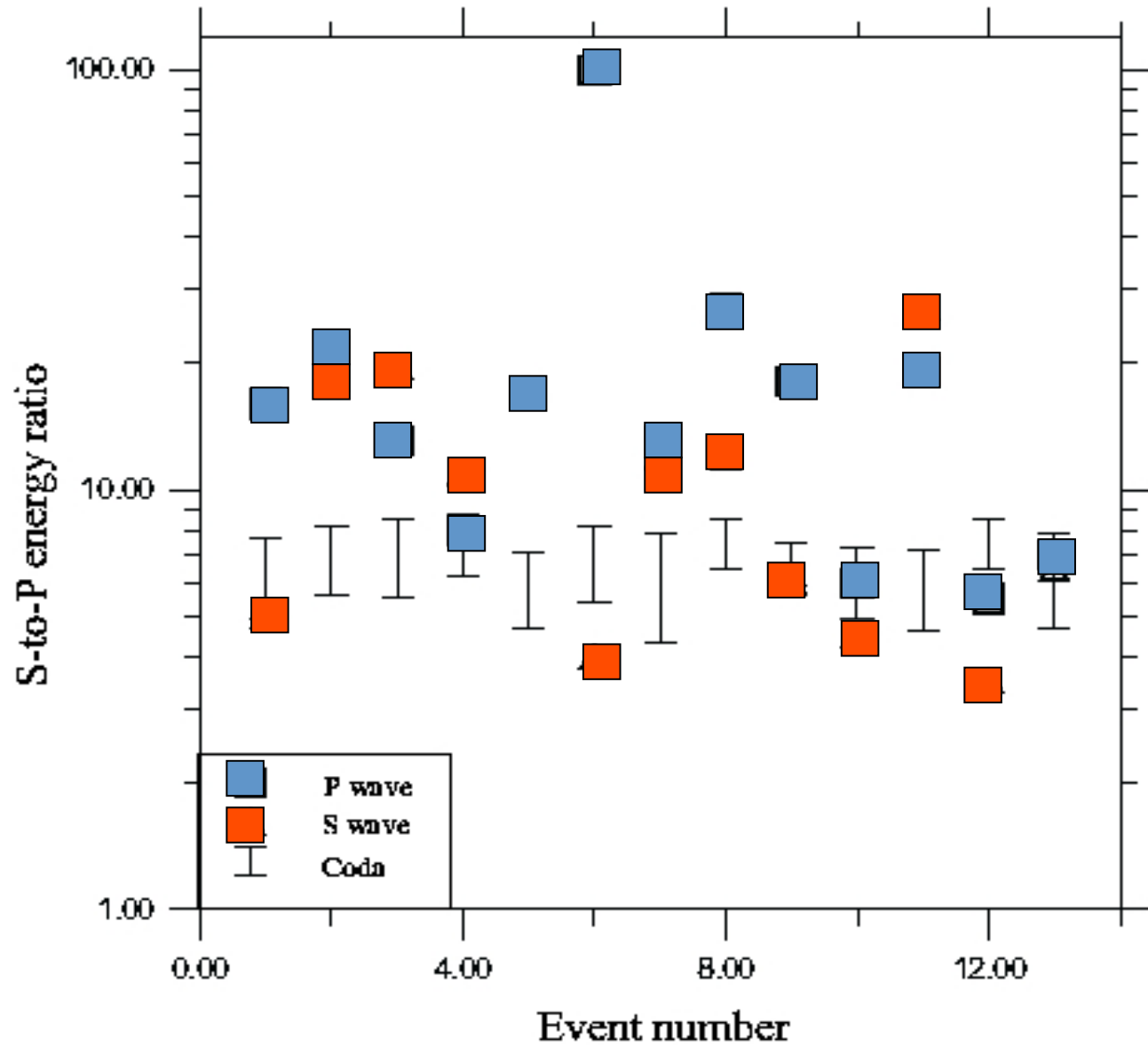


event 5



event 8





ENERGY RATIO	DATA	THEORY FULL SPACE	THEORY HALF SPACE BULK WAVES	THEORY HALF SPACE with RAYLEIGH WAVES
S/P	7.3	10.39	9.76	7.19
K/(S+P)	0.65	1	1.19	0.534
V(S+P)	-0.62	0	-0.336	-0.617



Model 1

Effect of a ‘thin’ layer: Love and Rayleigh

$$\alpha/\beta = \sqrt{3}$$

$\alpha = 2.77 \text{ km/s}$
 $\beta = 1.6 \text{ km/s}$
 $\rho = 2.7 \text{ km/s}$

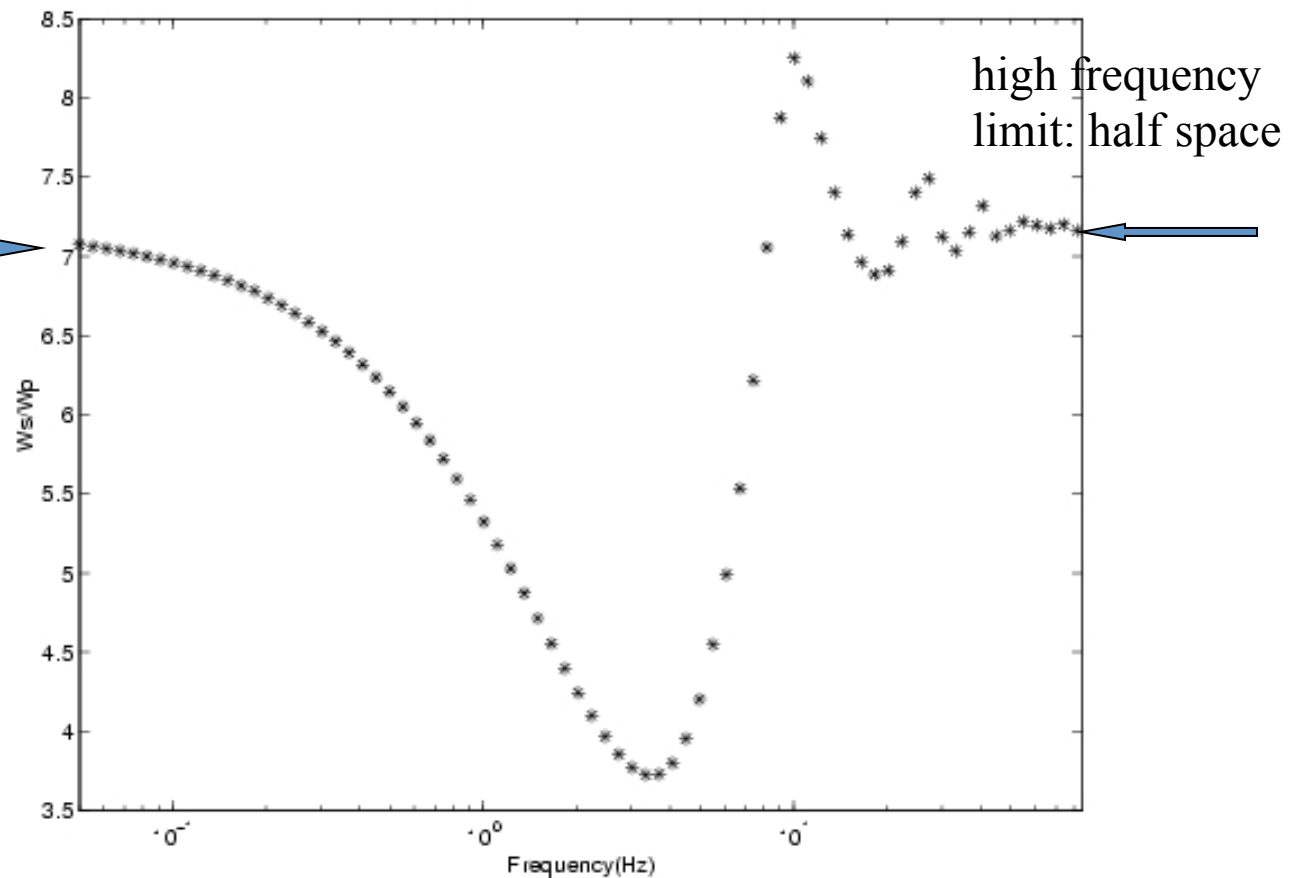
65 m

$$\alpha/\beta = \sqrt{3}$$

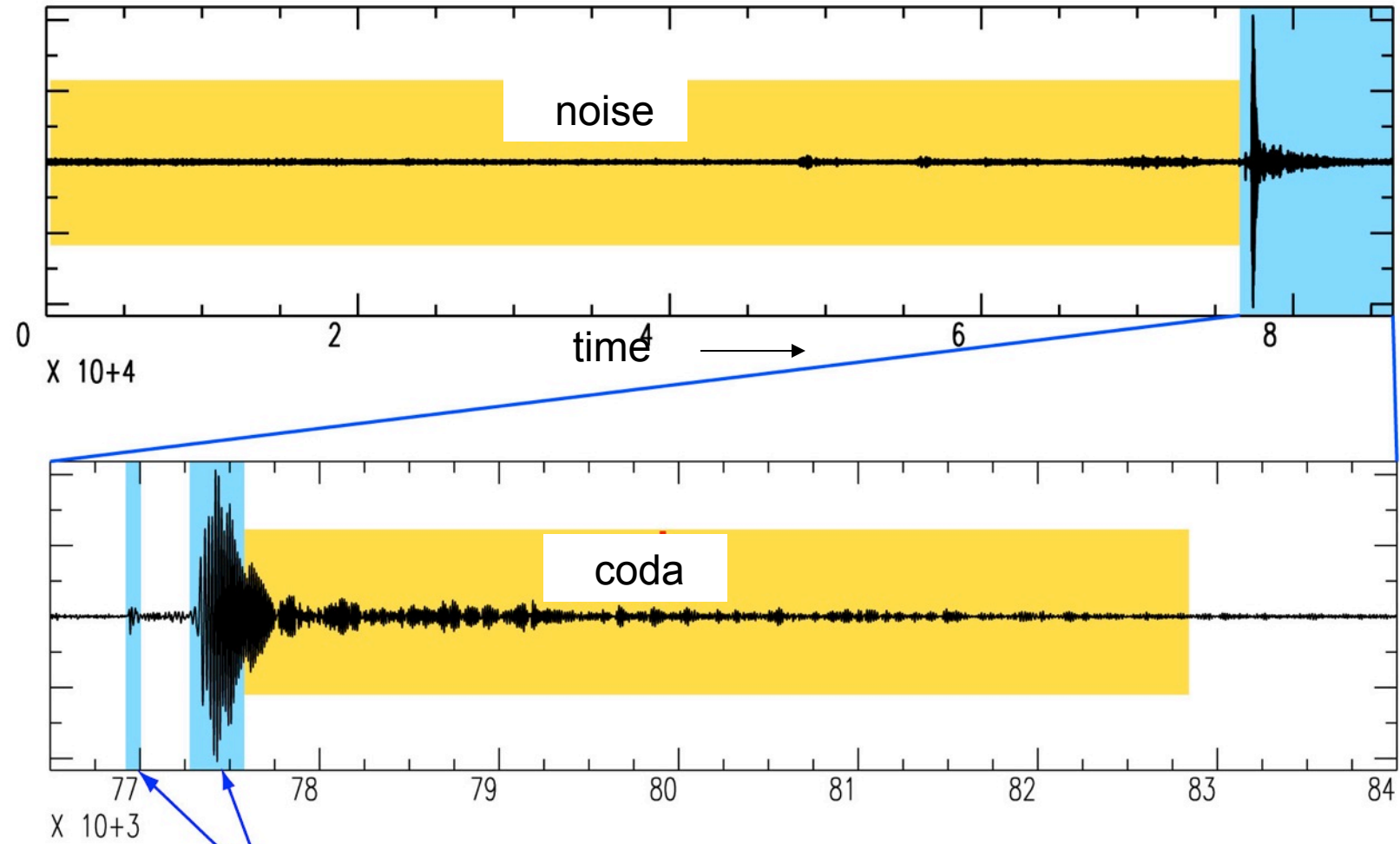
$\alpha = 5.2 \text{ km/s}$
 $\beta = 3 \text{ km/s}$
 $\rho = 2.7 \text{ km/s}$

low frequency
limit: half space

Margerin et al., 2009



Ground displacement

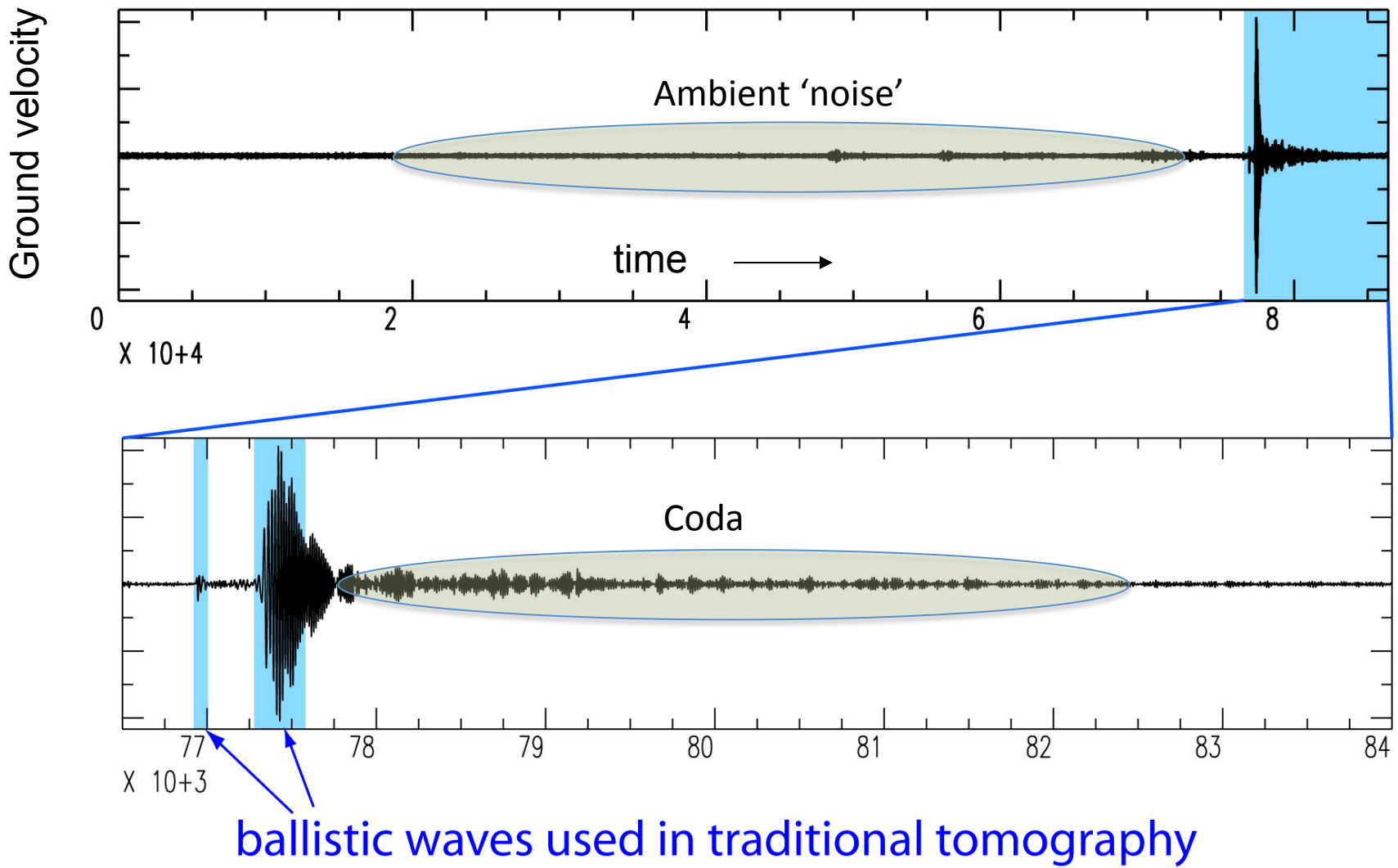


Direct waves

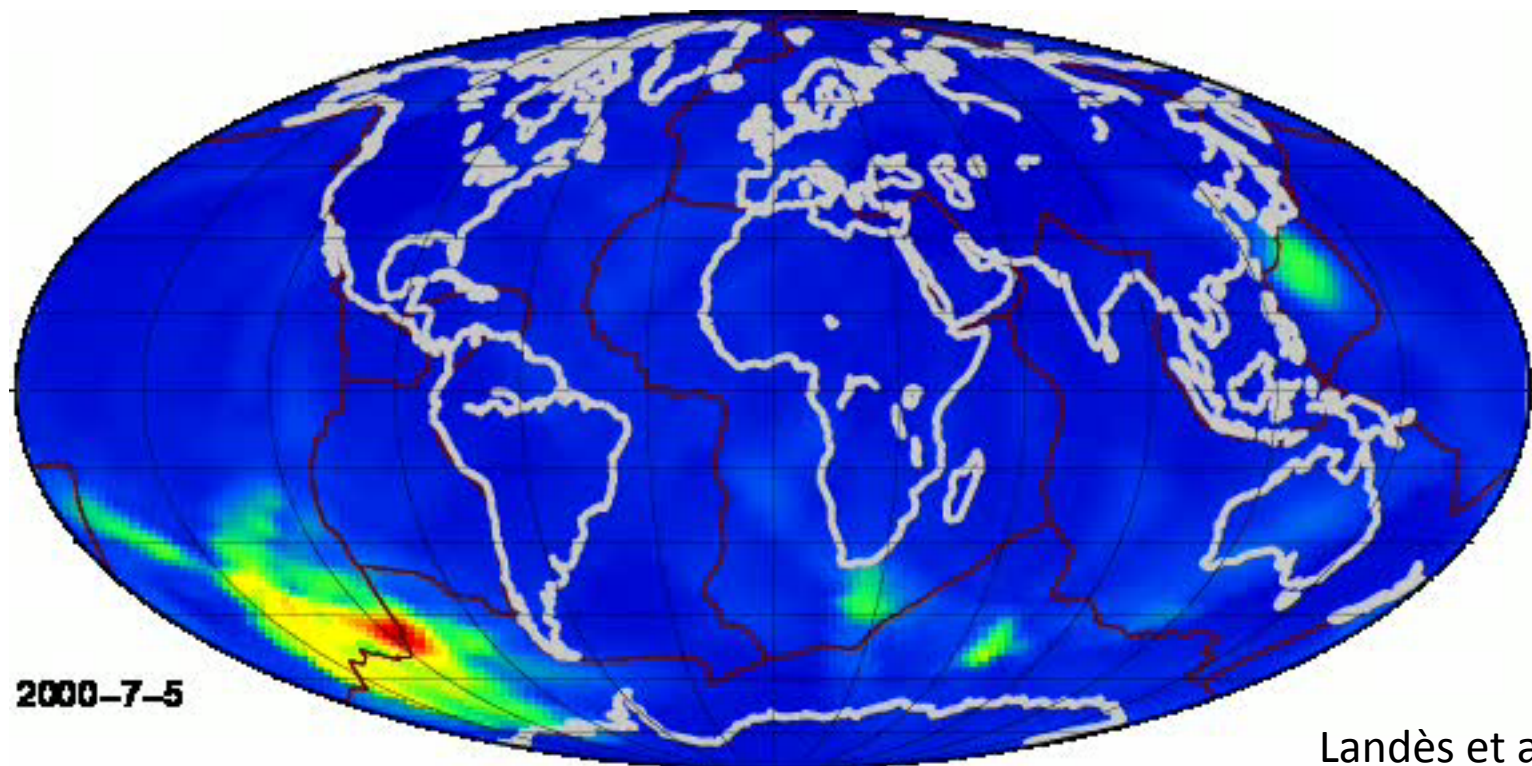
Ballistic waves used for imaging

'Noise' = no well-defined source (analogy with coda?)

one day of seismic record



The origin of the noise in the period band 5-10s as seen by seismic arrays



Landès et al., 2010

VARIABLE SOURCE LOCATIONS

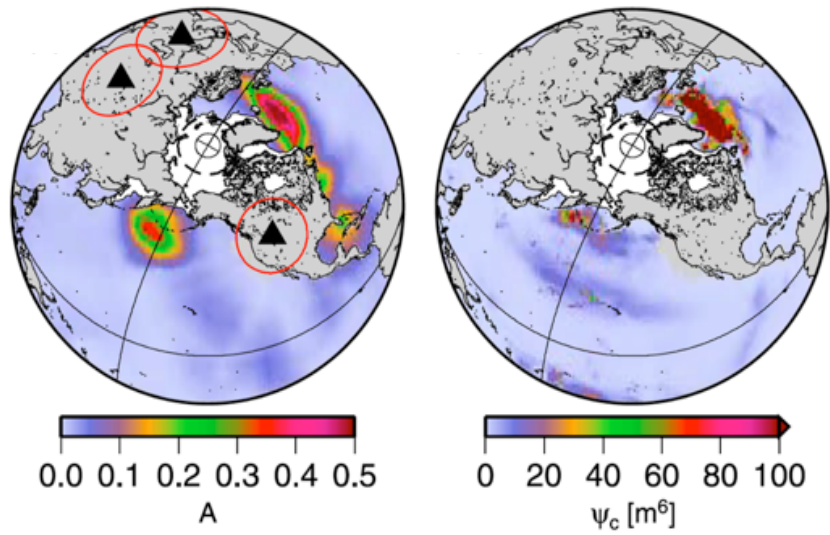
At higher frequencies: human activity, wind,....

Global ‘noise’ sources in the microseism band (extended \approx 2-50s)

Strong contribution from oceanic waves

Example of a global comparison
(secondary microseism-
Miche/Longuet-Higgins mechanism)

seismological observations oceanographic modeling



Hillers et al., 2012

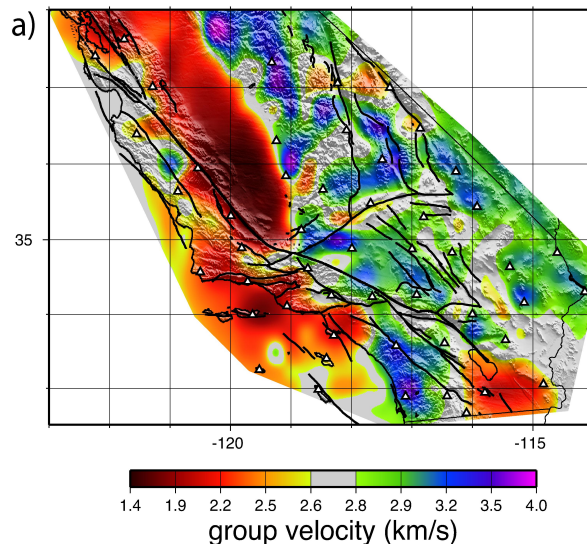
Longer periods: infragravity waves, e.g Fukao et al. 2010

+EARTHQUAKES

Cross-correlations of coda and noise records ≈ Green functions = virtual seismograms

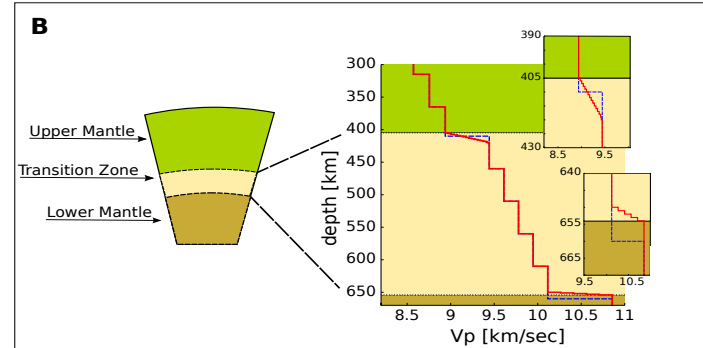
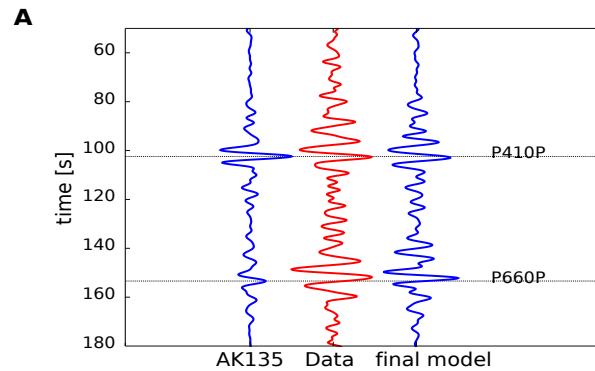
-demonstrated for the retrieval of surface waves (e.g. Paul and Campillo, 2001; Campillo and Paul, 2003; Shapiro and Campillo, 2004....) or body waves (e.g. Zhan et al., 2010 ; Poli et al., 2012).

High resolution velocity map of California obtained from ambient noise (Rayleigh)
(Shapiro, Campillo, Stehly and Ritzwoller, Science 2005)



Large N sensor array \Rightarrow $N^2/2$ correlations

**Earth's mantle discontinuities from ambient noise
(phase transition \rightarrow (P, T))**
Body waves (Poli et al., 2012)
Poli, Campillo, Pedersen. Science 2012



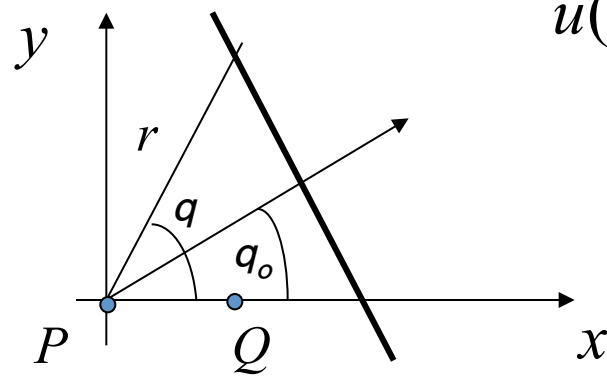
Aki (1957)

Evaluating k at different frequencies makes it possible to obtain the dispersion curve $C(\omega)$.

The method relies on the hypothesis of the stationnarity of the noise and requires specific array design to perform the azimuthal average.

Another approach consists of using only two points and to rely on long term average to produce the azimuthal average.

Let us consider a plane wave in 2D:



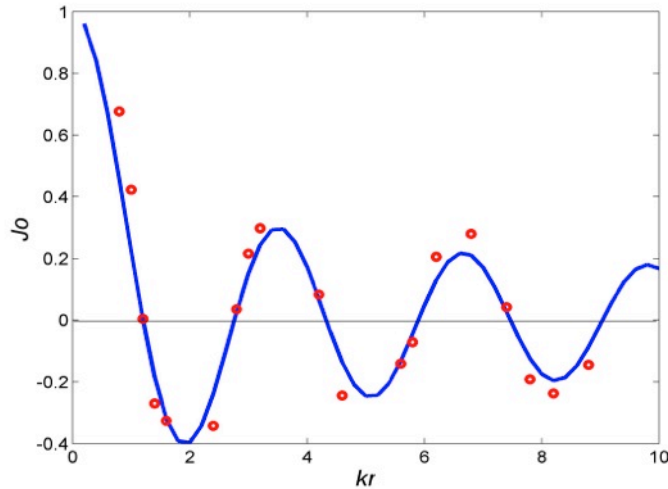
$$u(r, \theta, \omega) = F(\omega) \exp(-i k r \cos(\theta - \theta_0))$$

$$\frac{u^P u^Q^*}{|u^P| |u^Q|} = e^{+ikr \cos \theta_0}$$

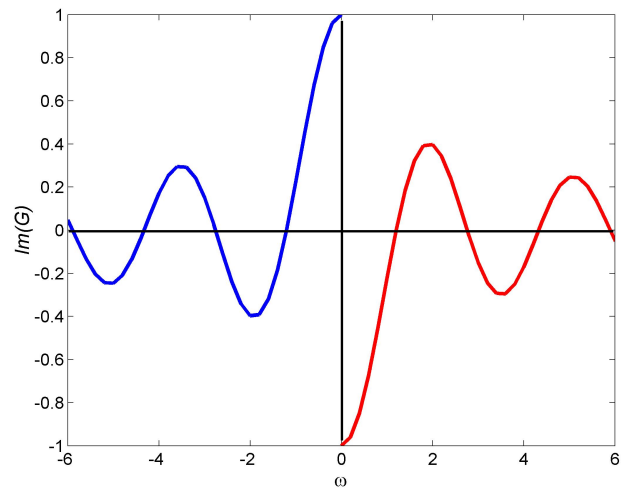
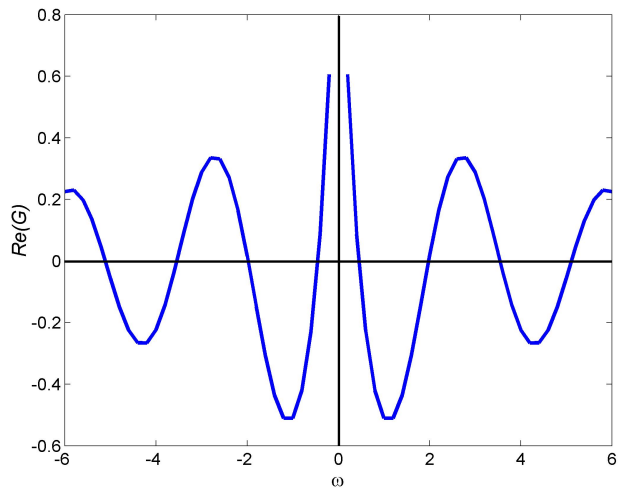
$$\langle \rho(r, \omega) \rangle = \left\langle \frac{u^P u^Q^*}{|u^P| |u^Q|} \right\rangle = \left\langle e^{ikr \cos \theta_0} \right\rangle = \frac{1}{2\pi} \int_0^{2\pi} e^{ikr \cos \theta_0} d\theta_0 = J_0(kr)$$

azimuthal average
of the spatial
cross-correlation

$$\frac{1}{2\pi} \int_0^{2\pi} \left(\sum_{m=0}^{\infty} \varepsilon_m i^m J_m(kr) \cos m\theta_0 \right) d\theta_0$$



$$G = \frac{1}{4i\mu} H_0^{(2)}\left(\frac{\omega r}{\beta}\right) = \frac{1}{4\mu} \left\{ -Y_0\left(\frac{\omega r}{\beta}\right) - i J_0\left(\frac{\omega r}{\beta}\right) \right\}$$

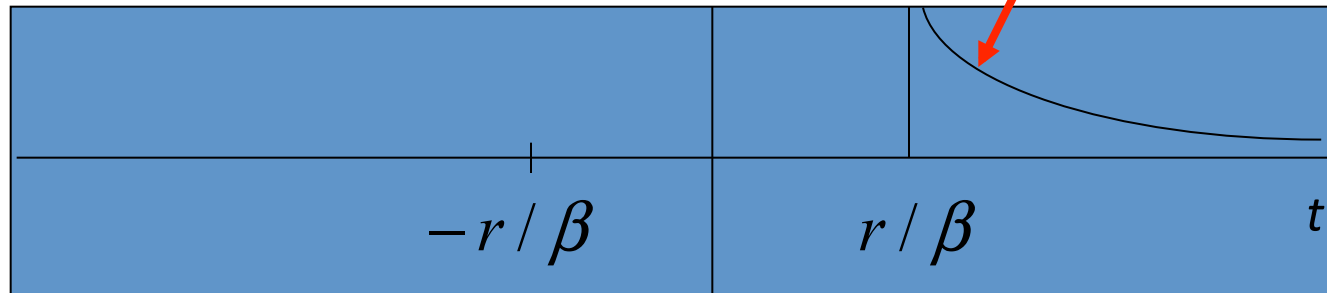


$$G(r,\omega) = \frac{-1}{4\mu} \left\{ \mathcal{H} \left[\operatorname{sgn}(\omega) J_0\left(\frac{\omega r}{\beta}\right) \right] + i \operatorname{sgn}(\omega) J_0\left(\frac{\omega r}{\beta}\right) \right\}$$

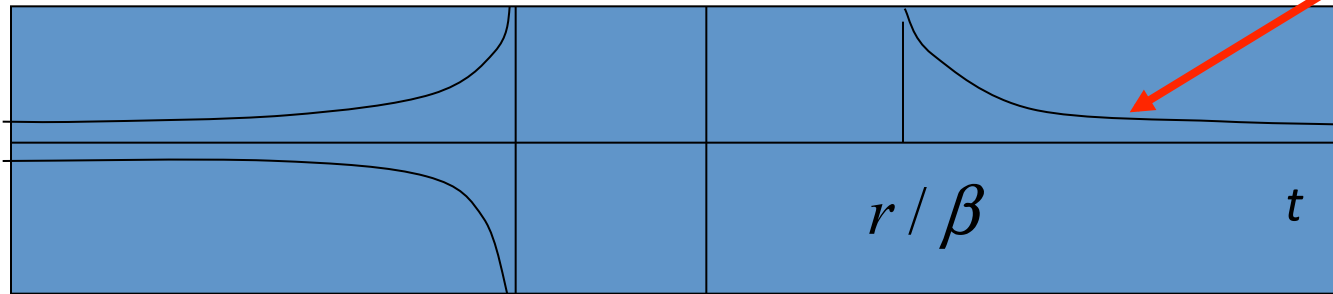
Causality

$$G = \frac{1}{4i\mu} H_0^{(2)}\left(\frac{\omega r}{\beta}\right)$$

$$G = \frac{1}{2\pi\mu} \frac{H\left(t - \frac{r/\beta}{\sqrt{t^2 - r^2/\beta^2}}\right)}{\sqrt{t^2 - r^2/\beta^2}}$$



(Re)
(Im)



$G/2$

(Im, Re)

$$G_{22}(r,\omega)\!=\!\frac{1}{4\mu}\!\left\{-Y_0\!\left(\frac{\omega r}{c}\right)\!-\!iJ_0\!\left(\frac{\omega r}{c}\right)\!\right\}$$

$$J_0\!\left(\frac{\omega r}{c(\omega)}\right)\!=\!-4\mu\operatorname{Im}\!\left(G_{22}(r,\omega)\right) \qquad\qquad r=|P,Q|$$

$$\operatorname{Im}\!\left(G_{22}^{PQ}\right)\!=\!\frac{-1}{4\mu}\!\left\langle\frac{u_2(P)u_2^*(Q)}{|u_2(P)\|u_2(Q)|}\right\rangle$$

P-SV case

Green function in 2D

$$G_{ij} = \frac{i}{4\rho\omega^2} \left\{ -\delta_{ij} k^2 H_0^{(2)}(kr) + \frac{\partial^2}{\partial x_i \partial x_l} [H_0^{(2)}(qr) - H_0^{(2)}(kr)] \delta_{lj} \right\}$$

$$G_{ij}(P, Q) = \frac{-i}{8\rho} \left\{ A \delta_{ij} - B (2\gamma_i \gamma_j - \delta_{ij}) \right\} \quad \gamma_j = \frac{x_j - \xi_j}{r}$$

$$A = \frac{H_0^{(2)}(qr)}{\alpha^2} + \frac{H_0^{(2)}(kr)}{\beta^2} \quad B = \frac{H_2^{(2)}(qr)}{\alpha^2} - \frac{H_2^{(2)}(kr)}{\beta^2}$$

$$\alpha = \sqrt{\frac{\lambda + 2\mu}{\rho}} \quad \beta = \sqrt{\frac{\mu}{\rho}} \quad r = |P, Q|$$

THE 2D VECTOR CASE

$$\beta^2 \frac{\partial^2 u_i}{\partial x_j \partial x_j} + (\alpha^2 - \beta^2) \frac{\partial^2 u_j}{\partial x_i \partial x_j} = \frac{\partial^2 u_i}{\partial t^2}$$

Summation of P and S plane waves:

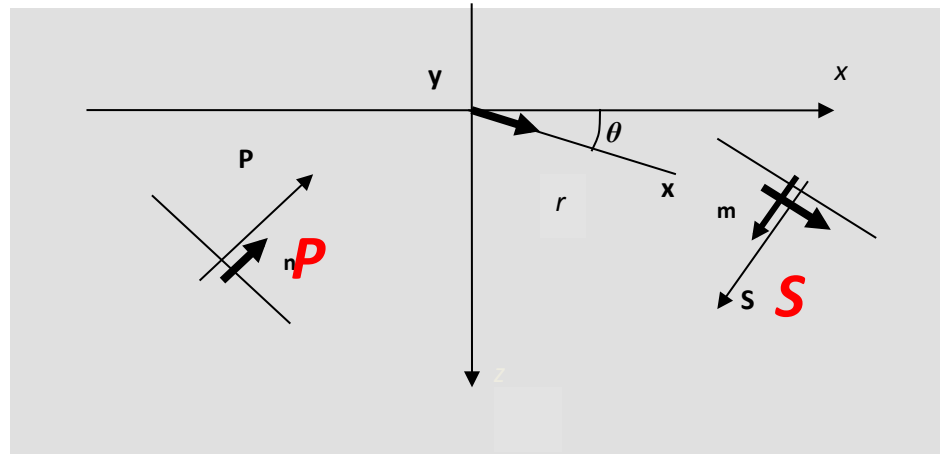
$$u_l(\mathbf{x}, \omega, t) = P(\omega, \phi) n_l \exp(-i \frac{\omega}{\alpha} x_j n_j) + S(\omega, \psi) m_l \exp(-i \frac{\omega}{\beta} x_j m_j)$$

Correlation:

$$u_l(\mathbf{y}) u_s^*(\mathbf{x}) =$$

$$(P^2 n_l n_s + S P^* m_l m_s) \exp(i k r \cos[\phi - \theta]) +$$

$$(S^2 m_l m_s + P S^* n_l n_s) \exp(i k r \cos[\psi - \theta])$$



Azimuthal average:

$$\langle \bullet \rangle = \frac{1}{4\pi^2} \int_0^{2\pi} d\phi \int_0^{2\pi} \bullet d\psi$$

$$\langle u_i(\mathbf{y}) u_j^*(\mathbf{x}) \rangle = \frac{S^2 \beta^2}{2} \{ A \delta_{ij} - B (2 \gamma_i \gamma_j - \delta_{ij}) \}$$

$$A = \varepsilon \frac{J_0(qr)}{\alpha^2} + \frac{J_0(kr)}{\beta^2} \text{ and } B = \varepsilon \frac{J_2(qr)}{\alpha^2} - \frac{J_2(kr)}{\beta^2}$$

And finally if $\varepsilon=1$

$$P^2 \alpha^2 = \varepsilon S^2 \beta^2$$

Equipartition ($\varepsilon=1$):

$$E_S / E_P = \left(\frac{\alpha}{\beta} \right)^2 \frac{1}{\varepsilon}$$

$$\langle u_i(\mathbf{y}, \omega) u_j^*(\mathbf{x}, \omega) \rangle \equiv -8E_S k^{-2} \operatorname{Im}[G_{ij}(\mathbf{x}, \mathbf{y}, \omega)]$$

Formally, same result in 3D (Sánchez-Sesma and Campillo, BSSA 2006)

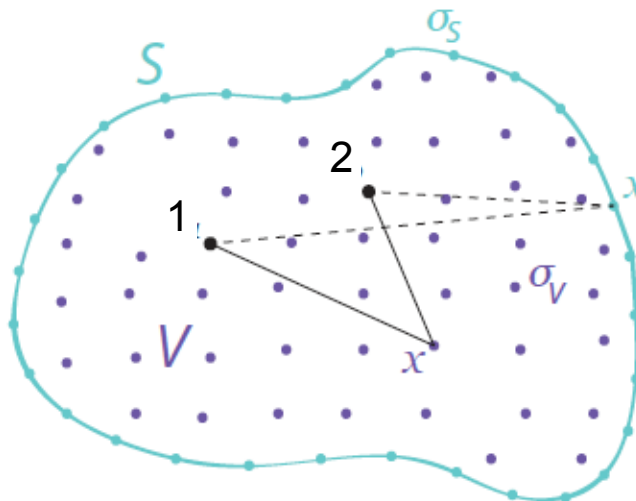
Arbitrary medium: an integral representation written in the frequency domain

(see e.g. Weaver et al. 2004, or Snieder, 2007)

$$G_{12} - G_{12}^* = \frac{4i\omega\kappa}{c} \int_V G_{1x} G_{2x}^* dV + \oint_S [G_{1x} \vec{\nabla}(G_{2x}^*) - \vec{\nabla}(G_{1x}) G_{2x}^*] d\vec{S}$$

Volume term Surface term





Helmholtz equation

$$G_{1x} = G(\vec{r}_1, \vec{x}; \omega)$$

$$\Delta G_{1x} + V(\vec{x}) G_{1x} + (k + i\kappa)^2 G_{1x} = \delta(\vec{x} - \vec{r}_1)$$

where the potential $V(\vec{x})$ describes the scattering contribution does not extend to infinity.

As for the classical representation theorem, we consider a combination of the fields from source at 1 and 2 and compute the flux:

$$I = \oint_S \left[G_{1x} \vec{\nabla} (G_{2x}^*) - \vec{\nabla} (G_{2x}) G_{1x}^* \right] \overrightarrow{dS}$$

With the divergence theorem:

$$I = \int_V \vec{\nabla} \left[G_{1x} \vec{\nabla} (G_{2x}^*) - \vec{\nabla} (G_{2x}) G_{1x}^* \right] dV$$

$$I = \int_{\mathcal{V}} \vec{\nabla} \left[G_{1x} \vec{\nabla} \left(G_{2x}^* \right) - \vec{\nabla} \left(G_{1x} \right) G_{2x}^* \right] dV \quad \text{reduces to}$$

$$I = \int_{\mathcal{V}} \left(G_{1x} \Delta G_{2x}^* - \Delta G_{1x} G_{2x}^* \right) dV$$

Using the definition of the GF:

$$\Delta G_{1x} = \delta(\vec{x} - \vec{r}_1) - V(\vec{x}) G_{1x} - (k + i\kappa)^2 G_{1x}$$

we obtain:

$$I = G_{12} - G_{21}^* - \frac{4i\omega\kappa}{c} \int_{\mathcal{V}} G_{1x} G_{2x}^* dV$$

and finally:

$$G_{12} - G_{12}^* = \frac{4i\omega\kappa}{c} \int_{\mathcal{V}} G_{1x} G_{2x}^* dV + \oint_S \left[G_{1x} \vec{\nabla} \left(G_{2x}^* \right) - \vec{\nabla} \left(G_{1x} \right) G_{2x}^* \right] \overrightarrow{dS}$$

Surface term:

$$G_{12} - G_{12}^* = \oint_S \left[G_{1x} \vec{\nabla} \left(G_{2x}^* \right) - \vec{\nabla} \left(G_{1x} \right) G_{2x}^* \right] d\vec{S}$$

$\kappa = 0$ (no attenuation)

No source in the bulk

Surface term:

$$G_{12} - G_{12}^* = \oint_S \left[G_{1x} \vec{\nabla} (G_{2x}^*) - \vec{\nabla} (G_{1x}) G_{2x}^* \right] \overrightarrow{dS}$$

If the surface is taken in the far field of the medium heterogeneities

$$G_{1x} \sim \frac{1}{4\pi |\vec{x} - \vec{r}_1|} \exp(-ik|\vec{x} - \vec{r}_1|) \text{ and } \vec{\nabla} (G_{1x}) \sim ik G_{1x}$$

and we obtain another widely used integral relation:

$$G_{12} - G_{12}^* = -2i \frac{\omega}{c} \oint_S G_{1x} G_{2x}^* dS$$

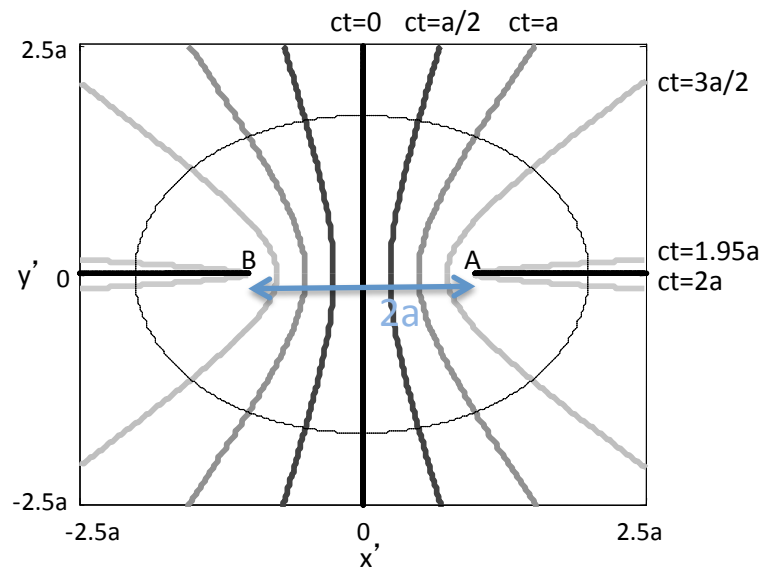
Volume term: $G_{12} - G_{12}^* = \frac{4i\omega\kappa}{c} \int_v G_{1x} G_{2x}^* dV$

κ is finite (attenuation)

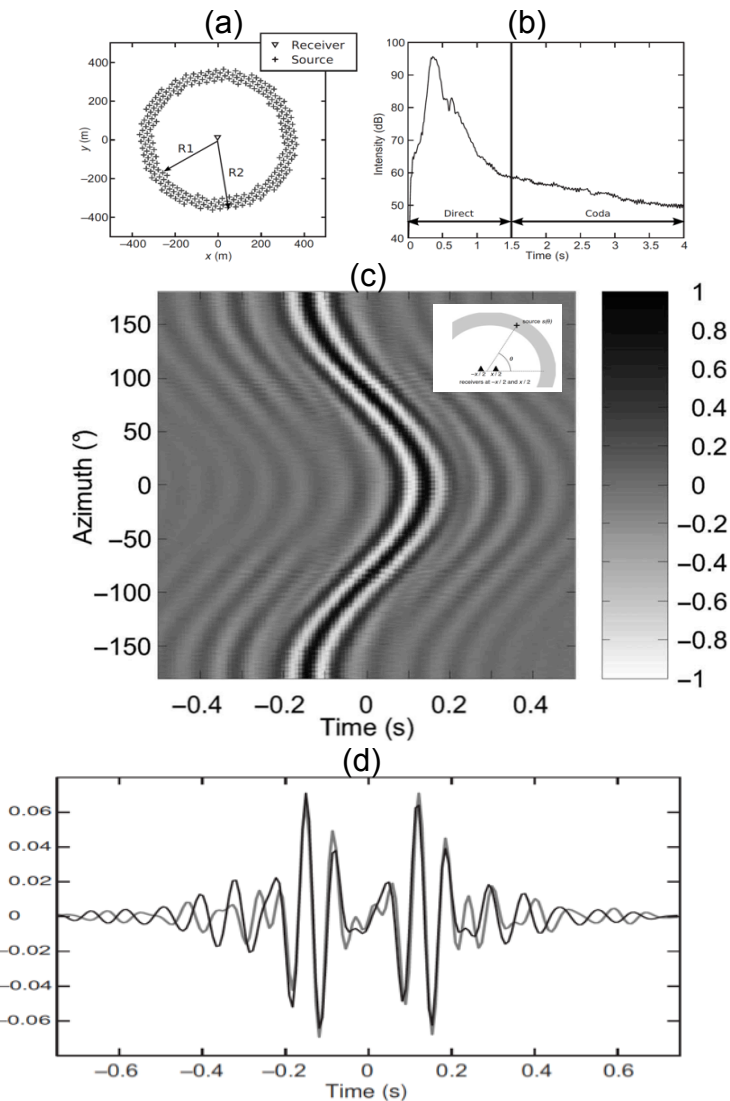
S is assumed to be sufficiently far away, for its contribution to be neglected (spreading and attenuation)

Location of the sources that contribute to the correlation: the end fire lobes

Difference of travel time between A and B
wrt the position of the source



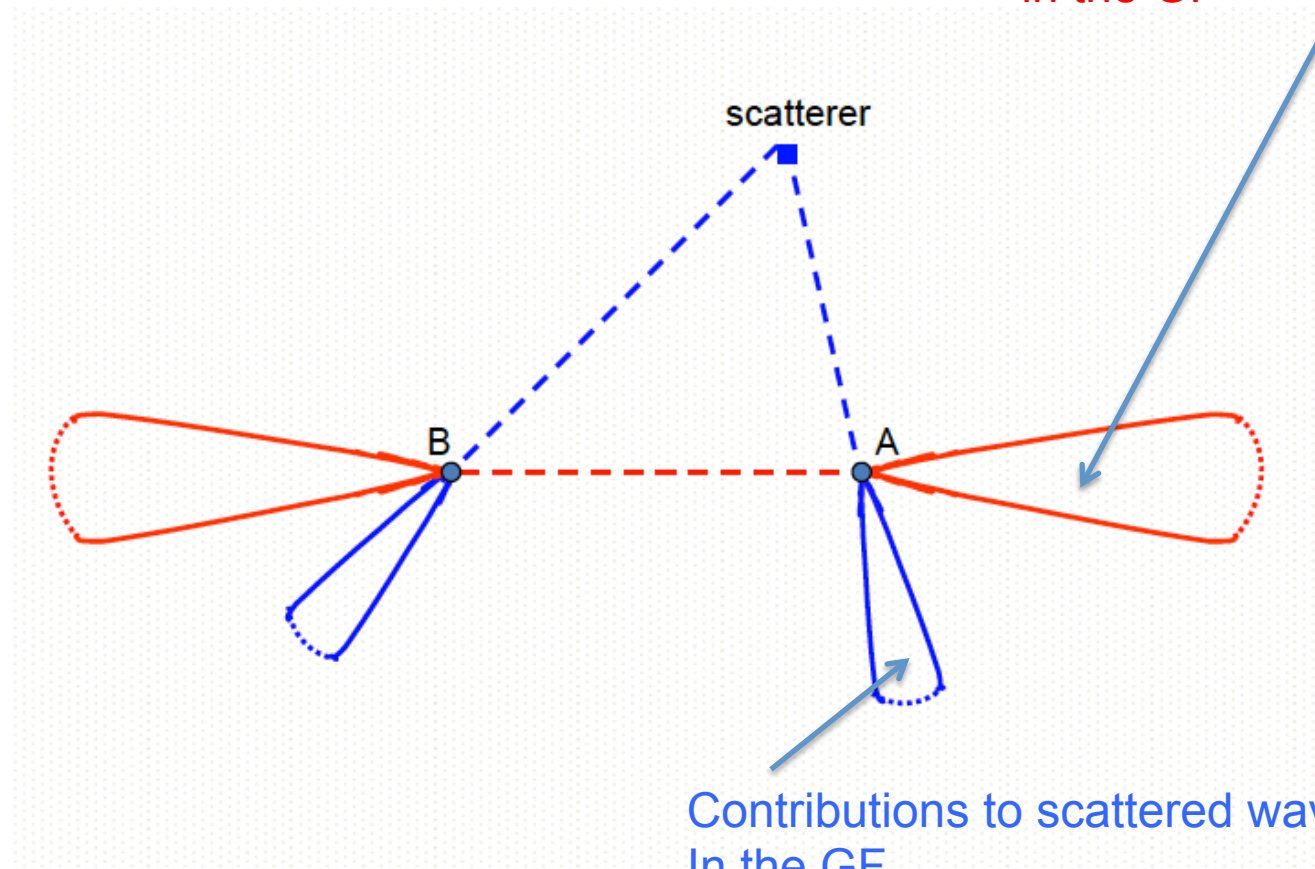
Stationary phase and end fire lobes



From Gouédard et al., 200X

End fire lobes

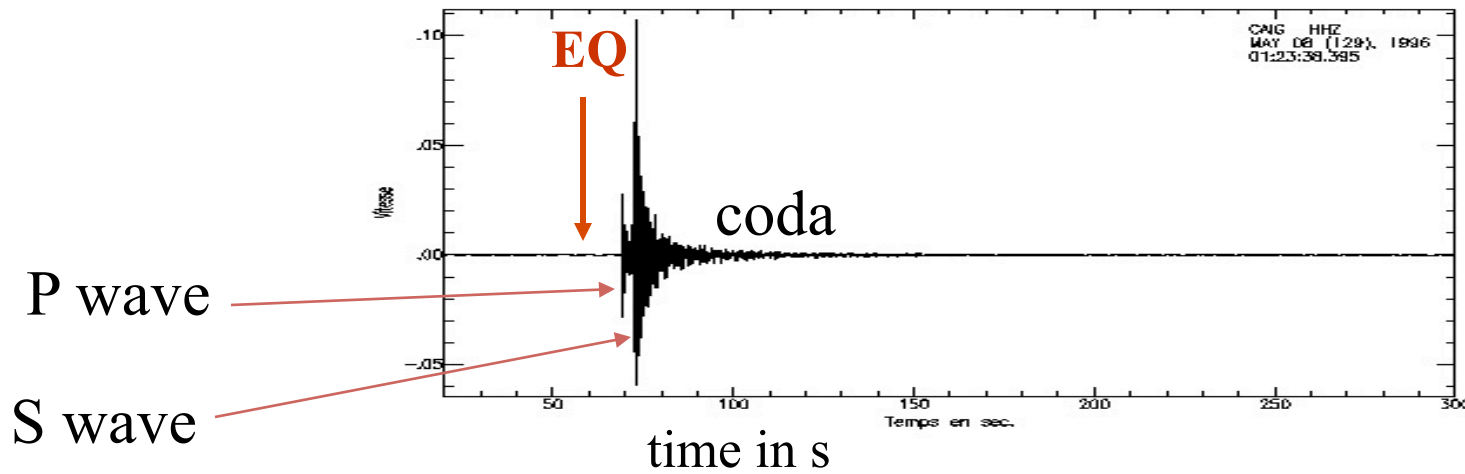
Contributions to direct waves
in the GF



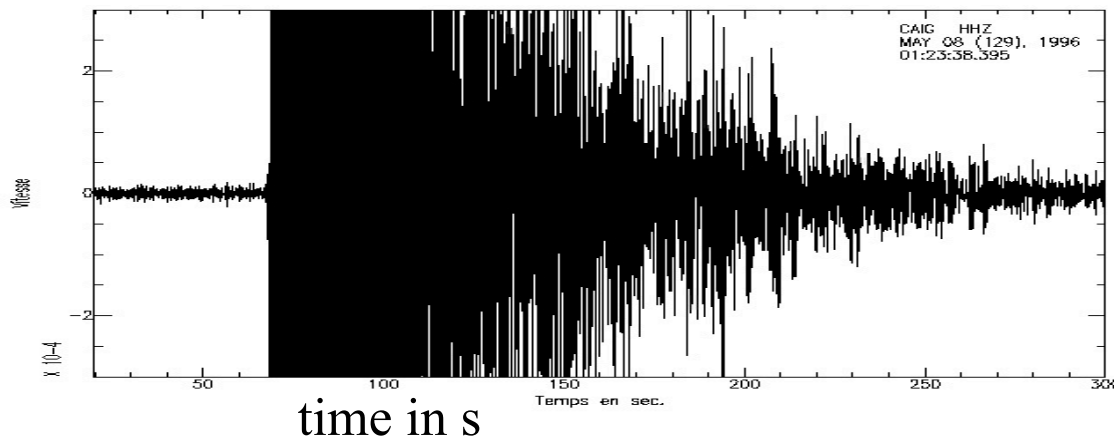
Contributions to scattered waves
In the GF

Extension to scattered waves

Correlations of coda records



scale x 1000:



An argument independant of the representation theorems

Multiple scattering and equipartition: the simplest case (finite body)

$$\phi(\vec{r}; t) = \sum_n a_n U_n(\vec{r}) \cos(\omega_n t)$$

Equipartition

All modes excited at the same level

$$\langle a_n a_m^* \rangle = F(\omega_n) \delta_{nm}$$

correlation

$$C_{1,2}(t) = \frac{1}{T} \int_0^T \phi(\vec{r}_1, \tau) \phi(\vec{r}_2, t + \tau) d\tau$$

Assuming a long recording interval T , this reduces to:

$$C_{1,2}(t) = \frac{1}{2} \sum_n F(\omega_n) U_n(\vec{r}_1) U_n(\vec{r}_2) \cos(\omega_n t)$$

Compare with:

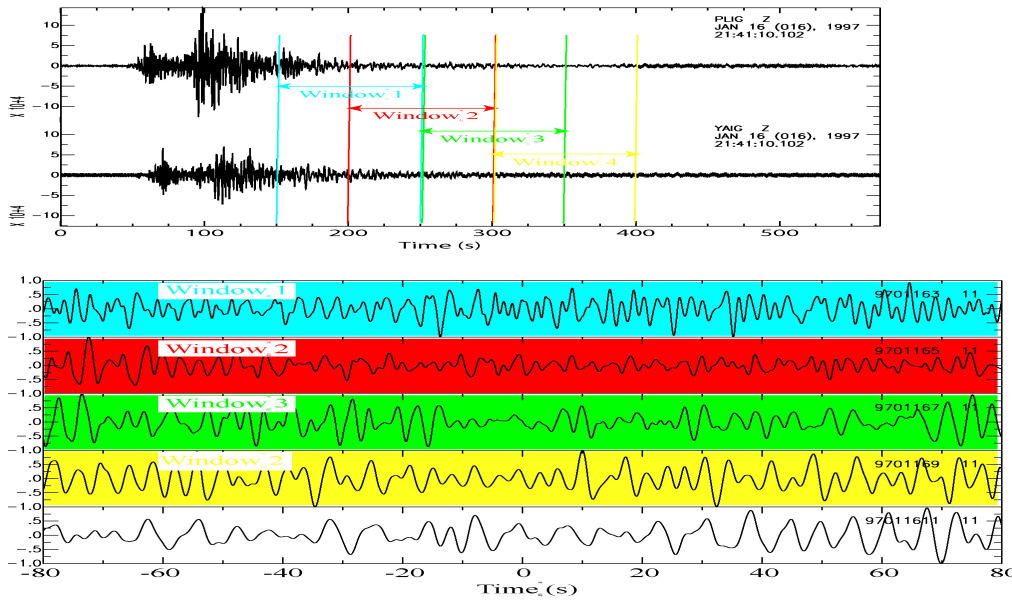
$$G(\vec{r}_1, \vec{r}_2; t) = \sum_n U_n(\vec{r}_1) U_n(\vec{r}_2) \frac{\sin(\omega_n t)}{\omega_n} \Theta(t)$$

1 derivative 2 causality

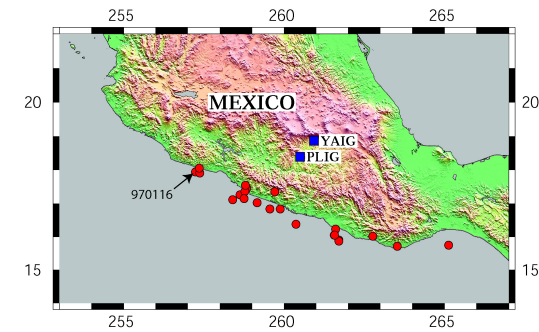
→ Long range correlation in seismic coda= Green function (*Paul and Campillo, AGU 2001, Campillo and Paul, Science 2003*)

Seismological application: coda waves

Individual cross-correlations: fluctuations dominate.

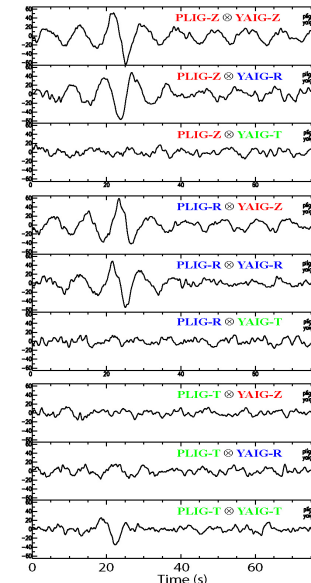


After averaging over 100 EQs →

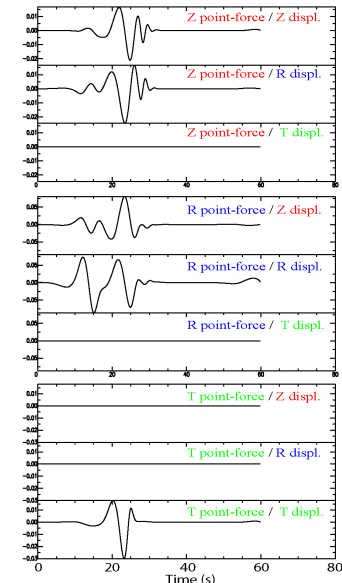


Emergence of the Green function

Stacks of 196 cross-correlations



Theoretical Green tensor at 69 km distance



Physical interpretations

Time reversal

MOVIE : revers_water



C source



Correlation and Time reversal Focusing/virtual source in A



C TR device

Equivalence in a reciprocal medium

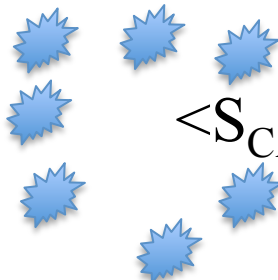


- C source
- A et B receivers

- Correlation :

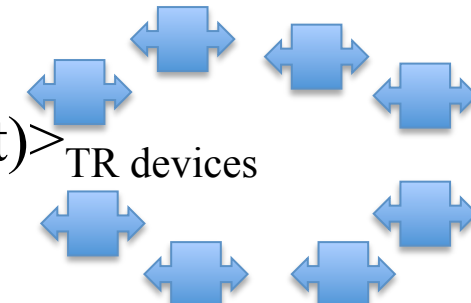
$$S_{CA}(t) \times S_{CB}(t)$$

- A source
 - C receiver ($S_{AC} = S_{CA}$)
 - C emits the time reversed signal
 - B receiver
 - Convolution :
- $$S_{CA}(t) \otimes S_{CB}(-t)$$



$$\langle S_{CA}(t) \times S_{CB}(t) \rangle_{\text{sources}}$$

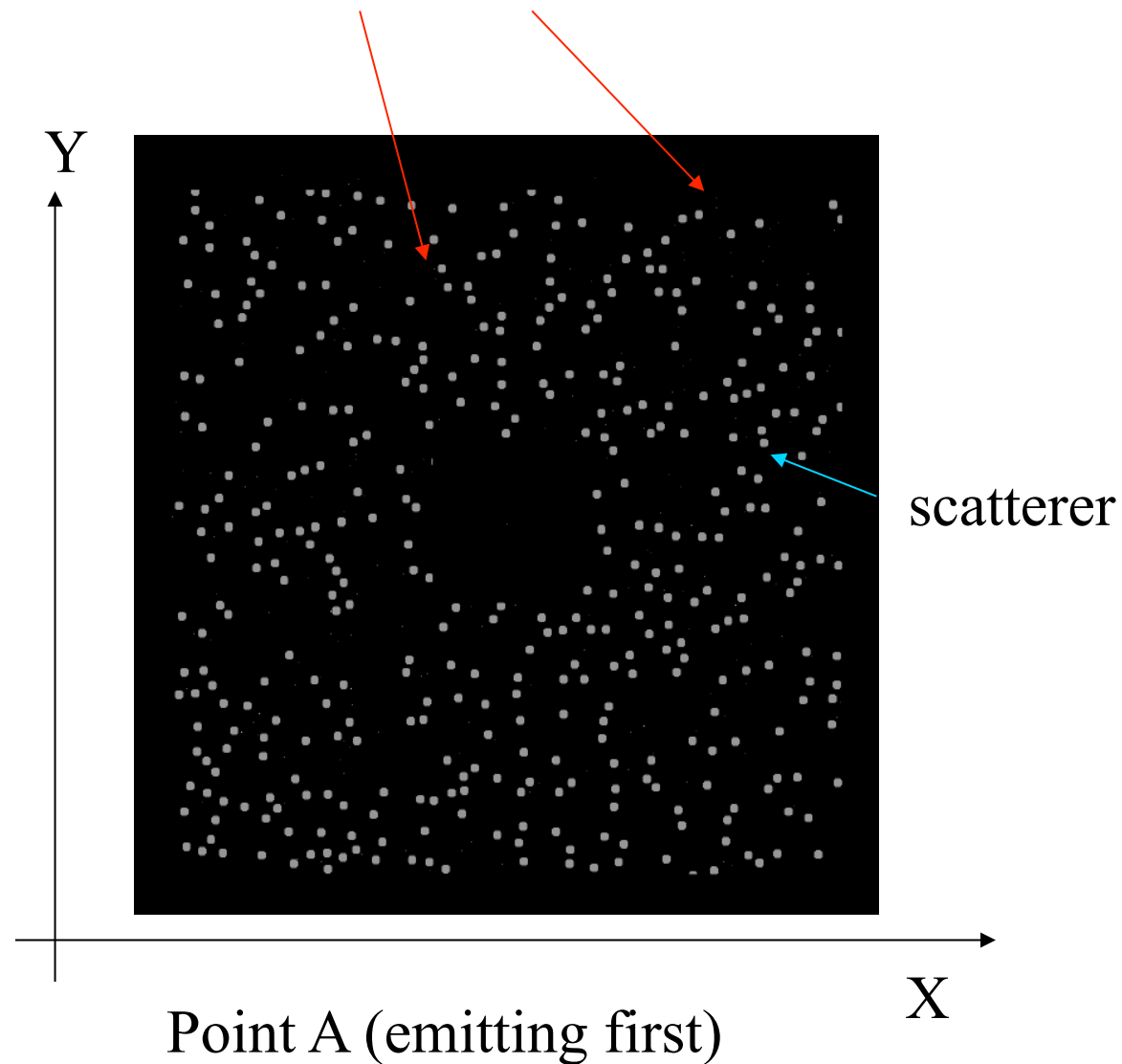
$$= \langle S_{CA}(t) \otimes S_{CB}(-t) \rangle_{\text{TR devices}}$$

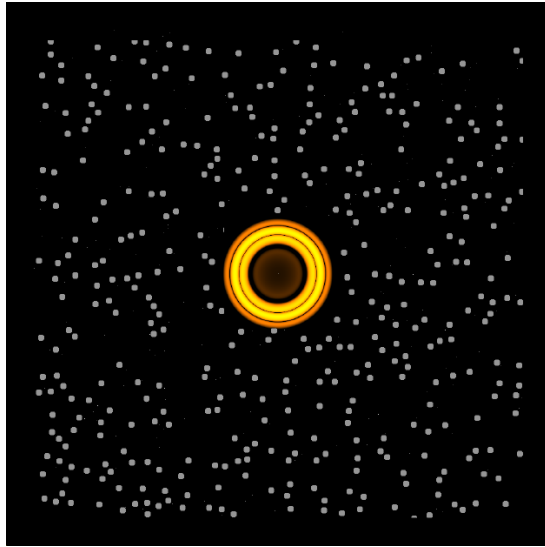


Ambient noise based method → using a (broken) time reversal mirror

Numerical 2D FD simulation

200 « sources » C (randomly placed)

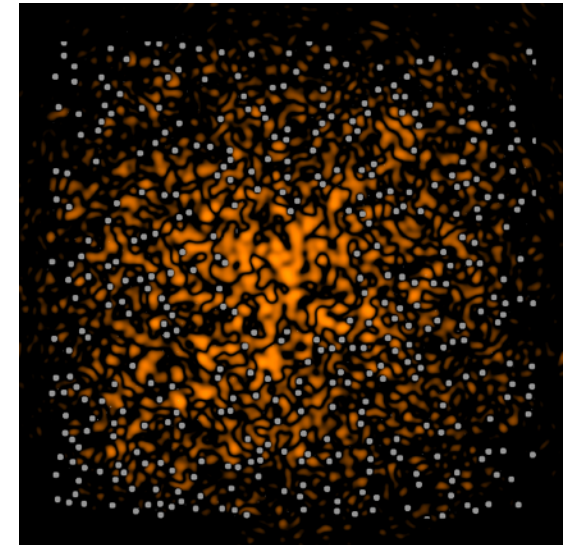


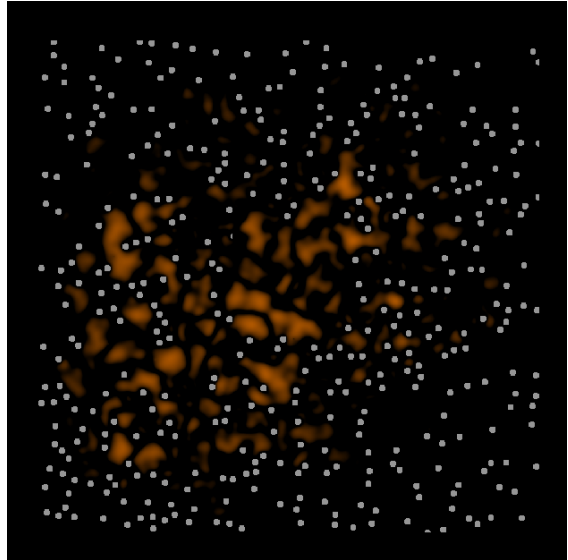


A pulse is emitted in A
and recorded at point randomly
distributed



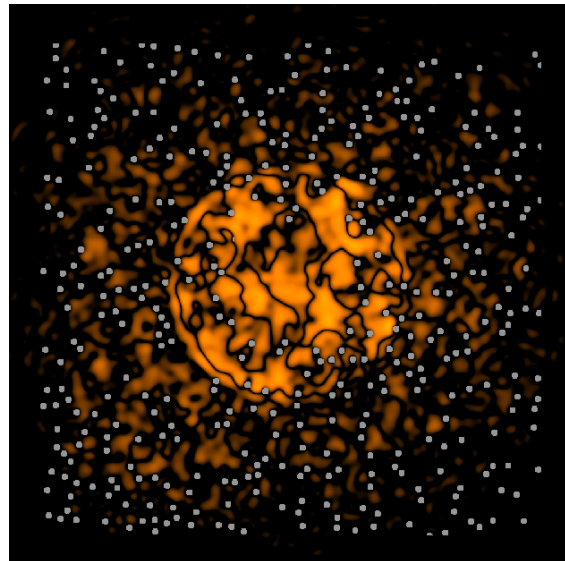
time



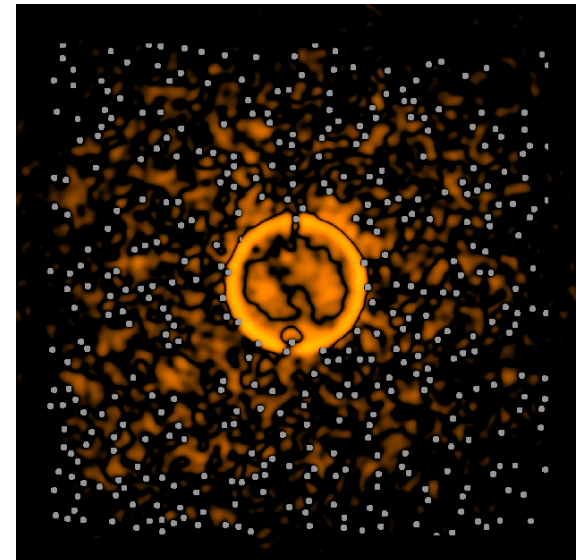


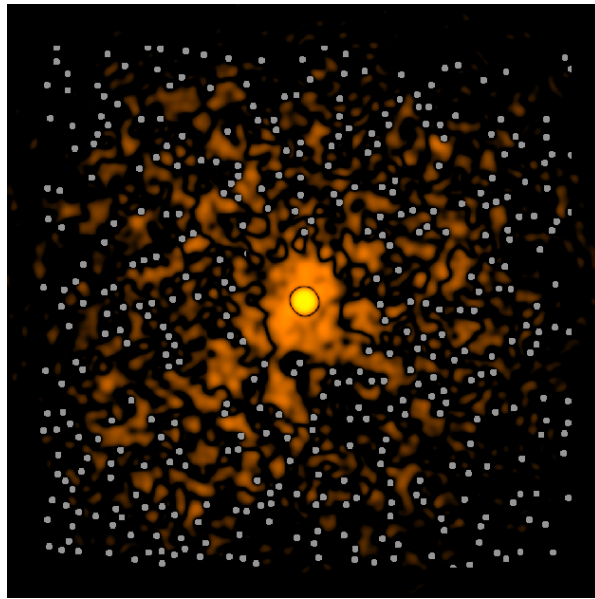
Constructive
interferences of time-
reversed field

Re-emission from the points ‘C’
of the time-reversed signals
(map of cross-correlations)



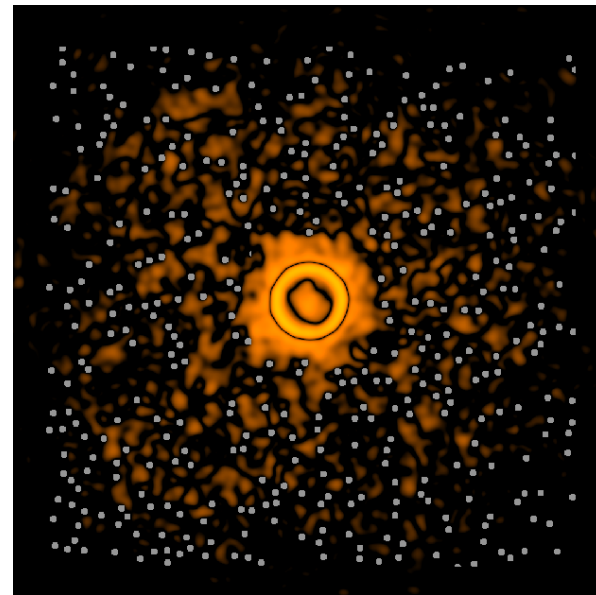
Converging field
 $: G(-t)$





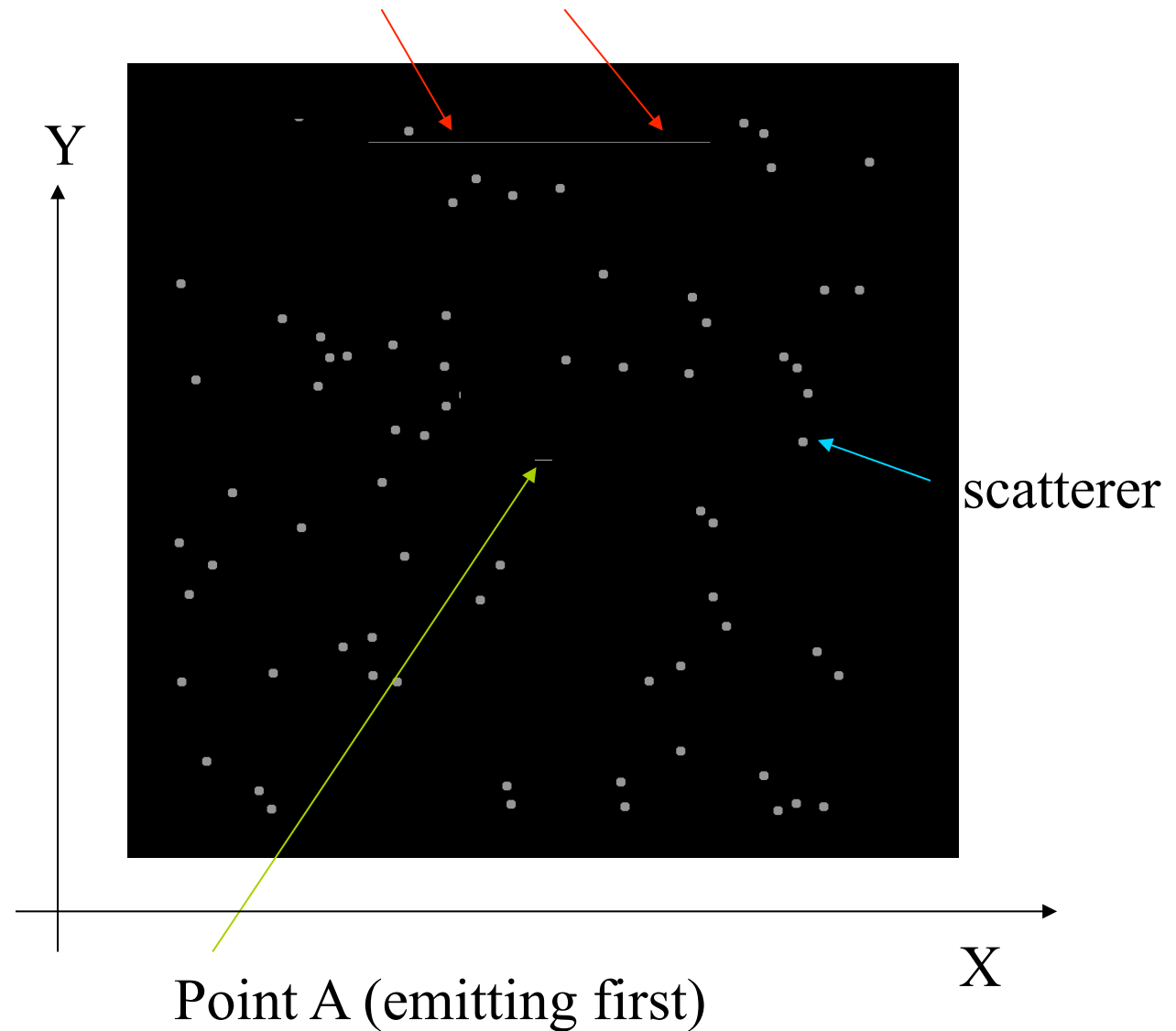
Nearly perfect refocalisation

Re-emission from A :
 $G(t)$

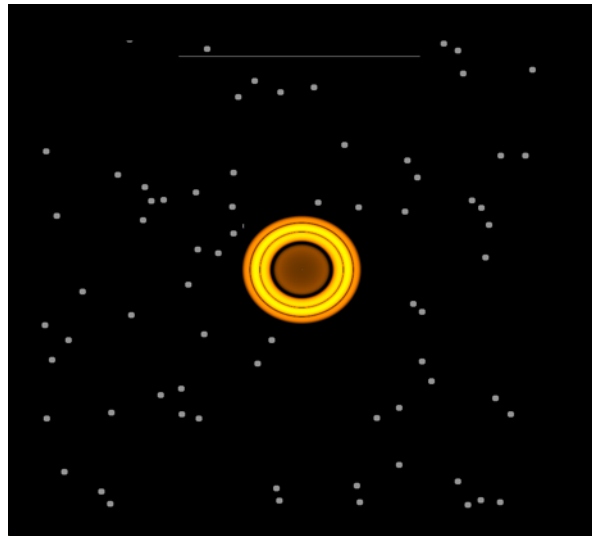


A more realistic configuration of sources

40 « sources » C (lined-up along a fault...)



Time reversal experiment

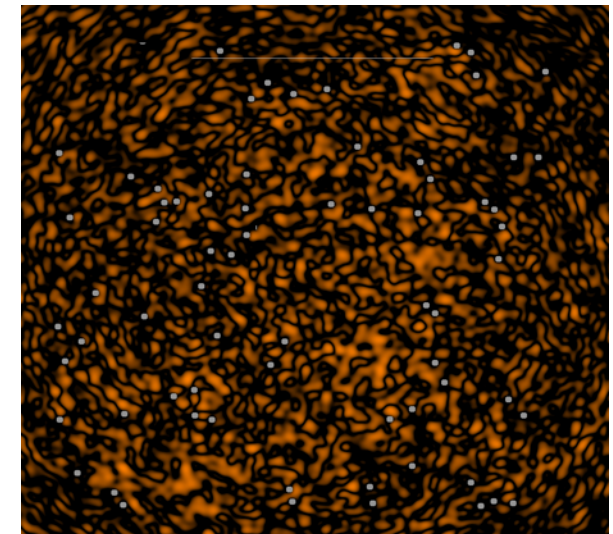


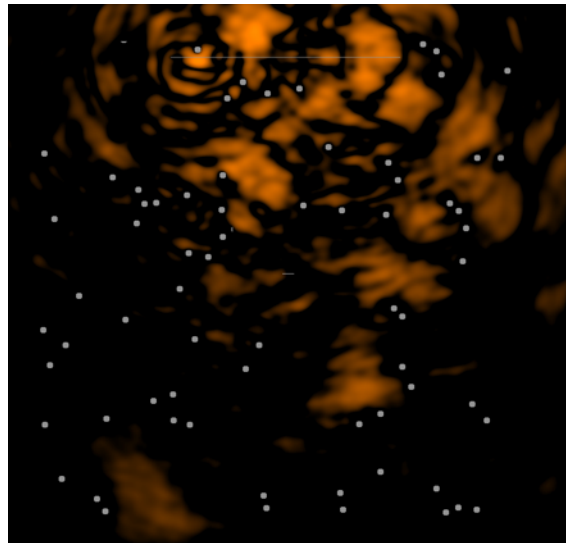
A send a pulse



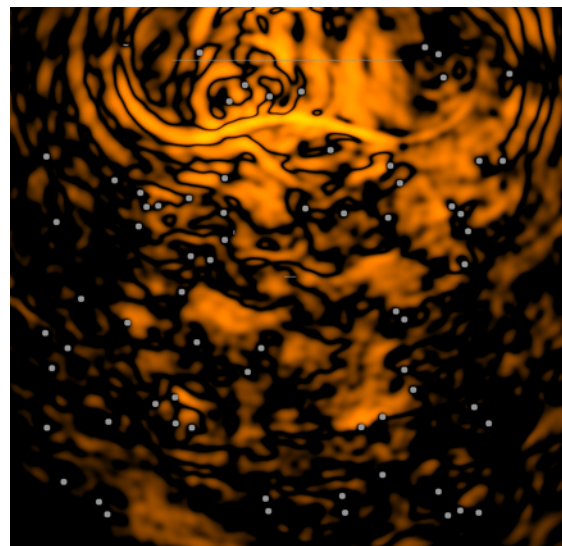
Scattering effects

Diffuse field is
also recorded



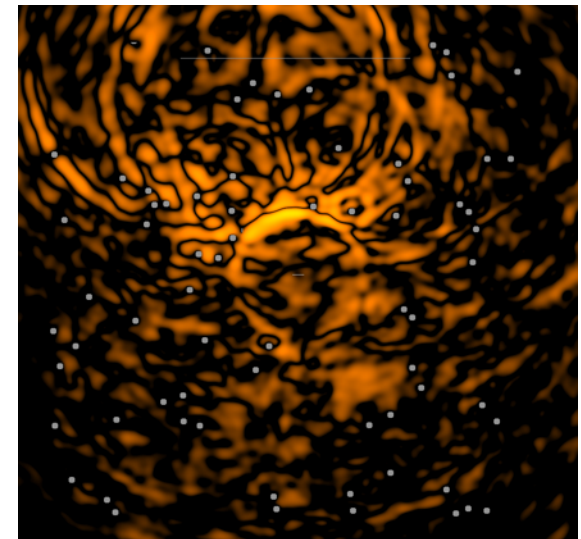


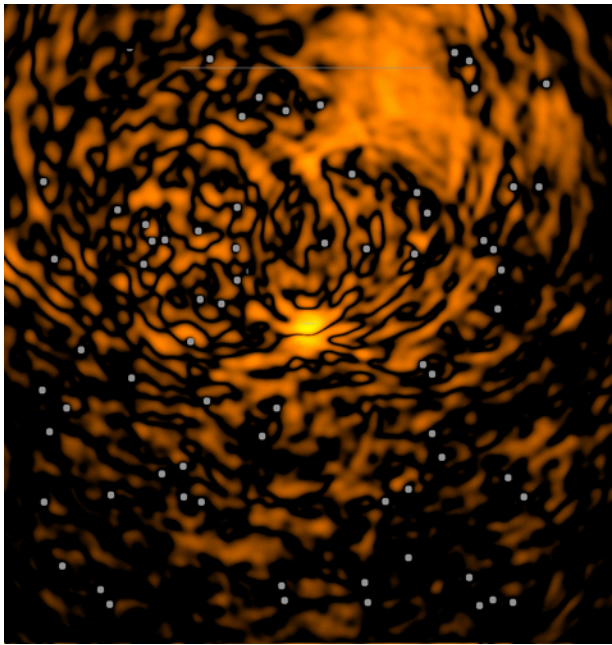
Re-emission



Converging field : $G(-t)$

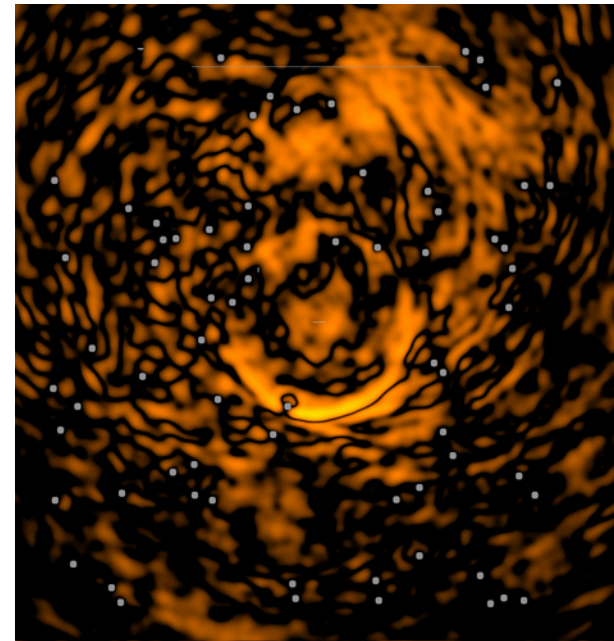
time





Partial focalisation

Diverging field : $h_{AB}(t)$



The symmetry of the Green function is lost!